Hepatic iron metabolism: studies on the regulation and function of Serine Protease Inhibitor clade B3 and Hemojuvelin

Patricia Catherine Kent

Division of Experimental Medicine, Department of Medicine
McGill University
Montreal, Quebec, Canada

December 2013

A thesis submitted to the School of Graduate Studies and Research of McGill University in partial fulfillment of the requirements of the degree of Master of Science

DEDICATION

I would like to dedicate this thesis to my mother Linda and siblings Alex, Alana, and Emma for their unwavering love and support.

ACKNOWLEDGMENTS

Firstly I would like to thank Dr. Kostas Pantopoulos for allowing me to pursue my graduate studies in his laboratory. I am truly grateful for his guidance and patience as my supervisor these past two years.

I must acknowledge the members of the Pantopoulos lab, both past and present for their day to day help, listening ears, laughter, and friendship. Specifically I must thank Dr. Carine Fillebeen, Mr. John Wagner, and Dr. Nicole Wilkinson. The three of them have been instrumental in my technical learning; from culturing cells, to molecular cloning, Western Blot troubleshooting, and mouse work. They never tired of my questions and constant lab commentary, for which I will forever remember them for fondly. Also, I want to say a special thank you to John for editing this thesis and Carine for her translation of the abstract.

I wish to thank my academic advisor Dr. Volker Blank and the members of my thesis committee Dr. Sam David and Dr. Sabah Hussain. Their support and suggestions in committee meetings were truly helpful in completing my projects.

For financial support I would like to express my gratitude to Dr. Kostas Pantopoulos, the Canadian Institute of Health Research (CIHR), the Division of Experimental Medicine at McGill University, and the Lady Davis Institute for allowing me to pursue my graduate studies at McGill University.

I also must thank all of my friends who have kept my sanity intact. Specifically I want to thank my Ultimate Frisbee team the Harshmellows, Nicole for Wednesday night dinner and movies, my PGSS trivia team, and all my friends who are only a phone call away.

I owe my brother Alex and sisters Alana and Emma a giant thank you. They have helped me stay positive and upbeat throughout my Masters, laughing with me as well as at me, and helping me to see the world beyond the lab.

To all the members of my immense immediate family, including my Willowburn Cr. family, I thank you for being the village that raised the child.

And lastly I owe this degree to my parents, Patrick and Linda Kent. After my father passed away, my mother continued to teach us children the power of independence, strength, and the importance of a good education. She has been a rock for the family and I will always be grateful for her tough love and support.

CONTRIBUTION OF AUTHOURS

The following thesis is structured in the manuscript-based format that complies with the guidelines set out by McGill University for thesis preparation. It consists of a manuscript in preparation, in which the candidate is the co-first author.

Chapter 1 is an introduction to iron research, presenting an overview of the topic via an extensive literature review of the current knowledge in the field. As well, a more focused introduction and rational of the study is provided at the beginning of each chapter.

Chapter 2 encompasses the first project entitled "Iron regulation of SERPIN B3 mRNA *in vitro* and its function in iron homeostasis". This data is part of a collaborative project with Dr. Patrizia Pontisso, whose laboratory performed the *in vivo* studies. All other experiments and data analysis were performed by P. Kent under the supervisory guidance and support of Dr. K. Pantopoulos.

Chapter 3 encompasses the second project undertaken entitled "A novel HFE and HJV double knockout mouse demonstrates crosstalk between the proteins for induction of hepcidin". A manuscript is being prepared with the data currently. Experiments, data analysis, and manuscript preparation were performed jointly between P. Kent and M. Constante. All figures for the manuscript were generated by P. Kent. Dr. K. Pantopoulos and Dr. M. Santos provided supervisory guidance and support.

Chapter 4 provides a brief general discussion and the main conclusions of the research.

Chapter 5 is the list of references.

TABLE OF CONTENTS

DEDICATION....2
ACKNOWLEDGMENTS....3
CONTRIBUTION OF AUTHOURS....5
TABLE OF CONTENTS....6
LIST OF ABBREVIATIONS....9
LIST OF TABLES....12
LIST OF FIGURES....13
ABSTRACT....14
RÉSUMÉ....16

CHAPTER 1: **INTRODUCTION**....18
1.1 The Ancient History of Iron....19
1.2 Iron's Janus Face....19
1.2.1 Biological Functions....19
1.2.2 Toxicity....20
1.3 Iron Distribution in the Body....21
1.4 Iron Absorption into Enterocytes....22
1.4.1 Non-Heme Bound (Inorganic) Iron....23
1.4.2 Heme Bound Iron....23
1.5 Iron Export to the Plasma....25
1.6 Transferrin Cycle....25
1.7 Tissue Iron Utilization....27
1.7.1 Erythrocytes....27
1.7.2 Macrophages....27
1.8 Iron Storage....28
1.9 Systemic Iron Regulation....28
1.9.1 Hepcidin....28
1.9.2 Hepcidin and Ferroportin....30

1.10 Hepcidin Regulation 30
1.10.1 Serum Iron 30
1.10.2 Hepatic Iron 31
1.10.3 Inflammation 33
1.10.4 Erythropoiesis 33
1.11 Iron Misregulation 33
1.11.1 Iron Overload – Hereditary Hemochromatosis 34
1.11.2 Iron Deficiency – Anemias 35

CHAPTER 2: **Iron regulation of SERPIN B3 mRNA *in vitro* and its function in iron homeostasis** 37
2.1 PREFACE 38
2.2 ABSTRACT 39
2.3 INTRODUCTION 40
2.4 MATERIALS AND METHODS 43
2.4.1 Plasmid Construction 43
2.4.2 Cell Culture 45
2.4.3 Cell Culture Treatments 46
2.4.4 Luciferase Assay 46
2.4.5 qPCR 47
2.4.6 Stable Clones 47
2.4.7 Western Blots 48
2.4.8 Statistical Analysis 48
2.5 RESULTS 49
2.5.1 SERPIN B3 promoter shows weak activity *in vitro* 50
2.5.2 SERPIN B3 promoter is unresponsive to iron and oxidative stress *in vitro* 53
2.5.3 Endogenous SERPIN B3 is weakly expressed in cell lines and is non-responsive to iron *in vitro* 56
2.5.4 Does SERPIN B3 function as an upstream regulator of hepcidin? 57
2.6 DISCUSSION 59

CHAPTER 3: **A novel HFE and HJV double knockout mouse demonstrates crosstalk between the proteins for induction of hepcidin**.....63
3.1 PREFACE.....64
3.2 ABSTRACT.....65
3.3 INTRODUCTION.....66
3.4 MATERIALS AND METHODS.....69
3.4.1 Animals.....69
3.4.2 CBC Measurements.....70
3.4.3 Serum Biochemistry.....70
3.4.4 Ferrozine Assay.....70
3.4.5 Atomic Absorption Spectrometry.....71
3.4.6 qPCR.....71
3.4.7 Statistical Analysis.....72
3.5 RESULTS.....72
3.5.1 DKO mice resemble $HJV^{-/-}$ in serum and blood parameters.....72
3.5.2 Severe liver iron loading is seen in both $HJV^{-/-}$ and DKO mice fed a standard diet.....74
3.5.3 Serum parameters of the DKO mice continue to phenocopy $HJV^{-/-}$ mice when challenged with a high iron diet.....75
3.5.4 Hepcidin mRNA expression is severely attenuated in DKO mice, particularly when normalized to liver iron loading.....77
3.5.5 BMP6, SMAD7, and Id1 mRNA expression is attenuated in DKO mice.....80
3.6 DISCUSSION.....81

CHAPTER 4: **FINAL CONCLUSIONS**.....88

CHAPTER 5: **REFERENCES**.....91

LIST OF ABBREVIATIONS

ACD Anemia of Chronic Diseases

ANOVA Analysis of Variance

BMP Bone Morphogenetic Protein

BMPR Bone Morphogenetic Protein Receptor

CBC Complete Blood Count

cDNA Complementary Deoxyribonucleic Acid

CIP Calf Intestinal Phosphatase

CO_2 Carbon dioxide

$CoCl_2$ Cobalt (II) Chloride

Cp Ceruloplasmin

DcytB Duodenal cytochrome B

ddH_2O Double Distilled Water

DFO Deferoxamine

DMEM Dulbecco's Modified Eagle's Medium

DMT1 Divalent Metal Transporter 1

DNA Deoxyribonucleic Acid

EPO Erythropoietin

ERK Extracellular signal Regulated Kinase

FAC Ferric Ammonium Citrate

FBS Fetal Bovine Serum

FLVCR Feline Leukemia Virus, subgroup C, Receptor

FPN Ferroportin

Ft Ferritin

GAPDH Glyceraldehyde 3-Phosphate Dehydrogenase

GDF15 Growth Differentiation Factor 15

GOx Glucose Oxidase

H_2O_2 Hydrogen Peroxide

HAMP Hepcidin gene

HCC Hepatocellular Carcinoma

H-chain Heavy chain Ferritin

HCl Hydrochloric acid

HCP1 Heme Carrier Protein 1

Hepc Hepcidin

Heph Hephaestin

HFE Hereditary Hemochromatosis Protein High Iron

HH Hereditary Hemochromatosis

HIF Hypoxia Inducible Factor

HJV Hemojuvelin

HO-1 Heme Oxygenase 1

HRP Horseradish Peroxidase

hyg Hygromycin

Id1 Inhibitor of DNA binding 1, dominant negative helix-loop-helix protein

IL Interleukin

IRIDA Iron Refractory Iron Deficiency Anemia

JNK1 c-Jun NH_2-Terminal Kinase 1

L-chain Light chain Ferritin

luc Luciferase gene

MAPK Mitogen Activated Protein Kinase

mRNA Messenger Ribonucleic Acid

NTBI Non Transferrin Bound Iron

O_2 Molecular Dioxygen

$O_2^{\bullet -}$ Superoxide Anion

OH^- Hydroxide Anion

$OH^\bullet$ Hydroxide Radical

OS Oxidative Stress

PBS Phosphate Buffered Saline

PCR Polymerase Chain Reaction

PS Penicillin and Streptomycin

puro Puromycin

qPCR Quantitative real-time Polymerase Chain Reaction

RCL Reactive Center Loop

RIPA Radioummuniprecipitation Assay Buffer

RNA Ribonucleic Acid

ROS Reactive Oxygen Species

SCC Squamous Cell Carcinoma

SCCA1 Squamous Cell Carcinoma Antigen 1

SDS-PAGE Sodium Dodecyl Sulfate Polyacrylamide Gel Electrophoresis

SEM Standard Error Mean

SERPIN B3, SB3 Serine Protease Inhibitor, clade B3

SMAD Homologs of both the *Drosophila* protein, Mothers Against Decapentaplegic and the *C. elegans* protein SMA

STAT Signal Transducer and Activator of Transcription

STEAP3 Six Transmembrane Epithelial Antigen of the Prostate 3

TBE Tris Borate EDTA

TBT-T Tris Buffered Saline – Tween 20

TCA Trichloroacetic acid

tet Tetracycline

Tf Transferrin

TfR1 Transferrin Receptor 1

TfR2 Transferrin Receptor 2

TIBC Total Iron Binding Capacity

TMPRSS6 Transmembrane Protease 6, also known as Matriptase-2

TNFα Tumour Necrosis Factor α

TWSG1 Twisted Gastrulation Homologue 1

WT Wildtype

LIST OF TABLES

CHAPTER 1

Table 1.1: Iron misregulation resulting in iron overload (hereditary hemochromatosis (HH)) or iron deficiency (anemia) 35

CHAPTER 2

Table 2.1: Primer sequences for plasmid construction. 45

Table 2.2: Primer sequences for qPCR 47

CHAPTER 3

Table 3.1: qPCR gene specific primer sequences. 72

LIST OF FIGURES

CHAPTER 1

Figure 1.1: Fenton and Haber-Weiss reactions. 20
Figure 1.2: Iron distribution in the body. 22
Figure 1.3: Dietary iron uptake by the enterocytes of the intestinal duodenum. 24
Figure 1.4: Transferrin mediated uptake of iron into cells. 26
Figure 1.5: Systemic iron regulation is orchestrated by hepcidin. 29
Figure 1.6: Hepcidin regulation from iron, inflammatory, and erythropoiesis cues. 32

CHAPTER 2

Figure 2.1: SERPIN B3 is overexpressed in the livers of hemochromatotic mice and is regulated by dietary iron 49
Figure 2.2: SERPIN B3 promoter activity is weak in Huh7 cells 52
Figure 2.3: SERPIN B3 promoter treated with iron sources or chelator and oxidative stress agents shows only mild induction with hemin 54
Figure 2.4: SERPIN B3 is weakly expressed in cell lines. 56
Figure 2.5: Huh7-tTA cells stabily expressing HJV WT and G320V mutant cDNA. 58

CHAPTER 3

Figure 3.1: Serum and complete blood analysis of mice fed a standard iron diet 73
Figure 3.2: Liver iron content of mice on a standard iron diet. 74
Figure 3.3: Serum analysis of high iron diet challenged mice 76
Figure 3.4: Hepcidin mRNA expression and tissue iron loading in mice fed a high dietary iron diet. 78
Figure 3.5: BMP6, SMAD7, and Id1 mRNA expression in dietary iron challenged mice 81

ABSTRACT

In the human body as in all mammals, iron is an essential trace element. Despite its required presence for many biological functions, it is also toxic because of its labile oxidation states and ability to catalyze reactions. For this reason, tight control must be exerted to maintain iron in a bioavailable yet redox inert state. Also since mammals possess no regulated iron excretion mechanism, the dietary uptake of the metal must be tightly controlled as well. This ensures that there is enough iron for the body's needs yet not too much as to result in iron overload and the complications which arise from it.

On a systemic level, mechanisms have evolved to safely move iron throughout the body, between cells that utilize, recycle, and store it. At the forefront of this process is hepcidin, a peptide hormone orchestrating the body's systemic iron homeostasis. Hepcidin is in turn controlled via iron, such that a balance is achieved between utilization and storage of the metal. Despite the number of safeguards that have evolved to maintain homeostasis, complications can arise, which allow researchers to ask questions and find answers.

It was investigated in Chapter 2 how a serine protease inhibitor, SERPIN B3, is affected by iron *in vitro*. A causative link was determined *in vivo* in a mouse model between iron overload and hepatic SERPIN B3 expression. However, *in vitro*, the results could not be recapitulated at the level of transcription, despite looking at both primary and secondary effects of iron. Furthermore, it was not possible to prove or disprove that SERPIN B3 plays a role in hepcidin expression.

In Chapter 3, the investigation of the role of two proteins which are well established in the hepcidin regulatory pathways was conducted. A novel knockout mouse was generated combining deletions in both the hereditary hemochromatosis (HFE) and hemojuvelin (HJV) proteins and iron accumulation and hepcidin expression in this double knockout (DKO) were investigated. It was

shown that the DKO mice are phenotypically like HJV single knockout mice and that there is crosstalk between the two iron sensing pathways.

RÉSUMÉ

Comme chez tous les mammifères, le fer est un élément essentiel au corps humain. Malgré sa présence nécessaire à de nombreuses fonctions biologiques, il est également potentiellement toxique à cause de ses états d'oxydation labiles et de sa capacité à catalyser des réactions. Pour cette raison un contrôle sévère doit être exercé pour maintenir le fer dans un état redox inerte tout en étant disponible biologiquement. Les mammifères ne possédant pas de mécanisme régulé d'excrétion du fer, l'apport alimentaire de ce métal doit également être étroitement contrôlé. Cela permet de combler adéquatement les besoins du corps en fer tout en évitant la surcharge en fer et les complications qui en résultent.

Au niveau systémique, des mécanismes ont évolué pour déplacer le fer correctement partout dans le corps entre des cellules qui utilisent, recyclent ou stockent cet élément. En première ligne de ce processus se trouve l'hepcidine, un peptide hormone, orchestrant l'homéostasie du fer au niveau systémique. L'hepcidine est à son tour régulée par l'intermédiaire du fer, de manière telle que la balance est atteinte entre l'utilisation et le stockage de ce métal. Malgré la présence de nombreux systèmes de contrôle responsables de la maintenance de l'homéostasie, des complications peuvent apparaître qui permettent aux chercheurs de poser des questions et de trouver des réponses.

Dans le chapitre 2, il a été étudié comment la SERPINE B3, un inhibiteur de protéase à serine, est affectée *in vitro* par le fer. Un lien de cause à effet avait été déterminé entre la surcharge en fer et l'expression hépatique de la SERPINE B3 *in vivo* dans un modèle murin. Cependant, les résultats au niveau de la transcription n'ont pas pu être récapitulés *in vitro*, malgré la recherche d'effets primaires et secondaires du fer. De plus, il n'a pas été possible de prouver ou d'invalider que la SERPINE B3 joue un rôle dans l'expression de l'hepcidine.

Dans le chapitre 3, l'investigation du rôle de deux protéines qui sont bien établies dans les voies de régulation de l'hepcidine a été conduite. Un nouveau modèle de souris knock-out a été généré combinant les délétions de HFE (héréditaire hemochromatose protein) et de l'hémojuveline (HJV). L'accumulation du fer et l'expression de l'hepcidine ont été étudiées dans ce double knock-out (DKO). Il a été montré que les souris DKO sont phénotypiquement similaires aux souris knockout HJV et qu'il existe un lien entre les deux systèmes de détection du fer.

CHAPTER 1

INTRODUCTION

1.1 The Ancient History of Iron

Iron is an ancient element, forming shortly after the Big Bang that created the universe nearly 14 billion years ago [1]. It is the sixth most abundant element in the universe [2] as well as the most abundant element on Earth, found primarily in the inner and outer cores [1]. Humans have been utilizing iron in their tools and weaponry for more than three millennia, but it was not until the eighteenth century when its chemical and biological relevance were first gleaned. Antoine Lavoisier the "father of modern chemistry" made one of his most important discoveries with the aid of iron; determining that water was comprised of oxygen and hydrogen [3]. He was the first to demonstrate in his experiments reacting water and iron the important relationship between iron and oxygen, which is essential to aerobic biological life.

1.2 Iron's Janus Face

1.2.1 Biological Functions

Iron plays a critical role in a number of diverse biological functions. It can be incorporated into proteins or coordinated into their active sites where it functions as a cofactor for a variety of reactions. However, since iron is a transition metal with eight possible oxidation states, it rarely appears un-coordinated. It most often is a constituent of heme or coordinated with sulphur or oxygen [4]. For example, iron within heme is found within hemoglobin which allows mammals to transport oxygen [5] and heme is also present in the mitochondrial cytochrome C protein where it aids in electron transfer in the organelle [6]. Proteins containing sulphur- or oxygen- coordinated iron often have the metal playing a catalytic function. For example, the DNA synthesis enzyme ribonucleotide reductase, which is essential for DNA replication contains an iron-oxo center, and the citric acid cycle protein aconitase contains an iron-sulphur cluster [6].

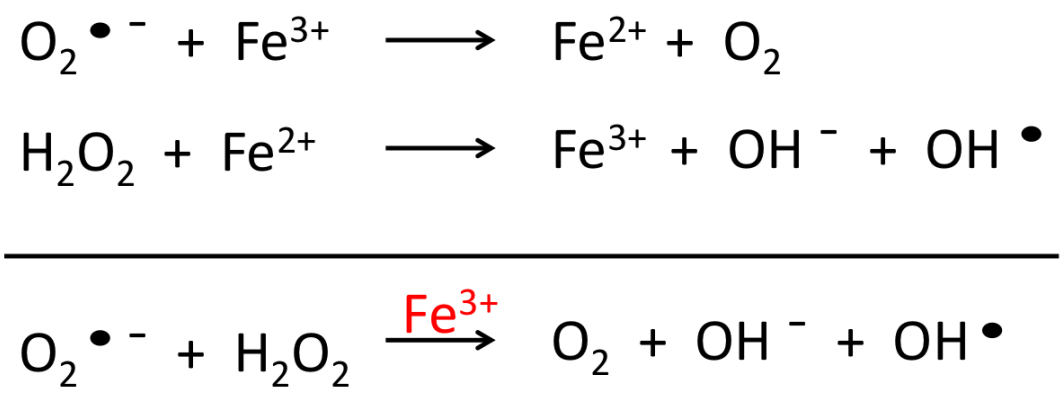

Figure 1.1: Fenton and Haber-Weiss reactions. Ferric iron catalyzes the generation of the hydroxyl radical ($OH^{\bullet}$) from the two reactive oxygen species (ROS) the superoxide anion ($O_2^{\bullet -}$) and hydrogen peroxide (H_2O_2) found in the mitochondria as by-products of cellular respiration.

1.2.2 Toxicity

Biologically, iron is essential for a number of metabolic and catalytic functions, but it is also toxic when 'free'. As mentioned iron is a transition metal and therefore can readily convert between its two commonly found oxidation states; Fe(II) (ferrous) and Fe(III) (ferric), by the transfer of one electron [7]. Therefore iron can be a catalyst, both accepting and donating an electron while remain unchanged over the course of a reaction. This characteristic is seen in the Fenton and Haber-Weiss reactions, where two reactive oxygen species (ROS); the superoxide anion ($O_2^{\bullet -}$) and hydrogen peroxide (H_2O_2), in the presence of free ferric iron are converted into the hydroxide anion (OH^-), molecular dioxygen (O_2), and the highly reactive ROS; the hydroxyl radical ($OH^{\bullet}$) [8, 9] (Figure 1.1). This reaction is biologically relevant since these ROS are present within the mitochondria as by-products of cellular respiration [6]. Since iron is also present in the mitochondria, it must be shielded to prevent the generation of the highly reactive hydroxyl radical which can cause oxidative stress (OS) to damage lipids, DNA, and proteins [10-12].

1.3 Iron Distribution in the Body

However potentially toxic iron can be, it is also an essential element in the human body (Figure 1.2). The average healthy adult has about 45-55mg of iron per kilogram, resulting in 3-5 grams of total iron [13]. This makes iron the most abundant transition metal in the body and it is constantly being recycled since there is no regulated iron excretion mechanism [14]. Iron is only lost via sloughing of epithelial cells from the skin or intestinal tract, blood loss, and through sweating [15]. Daily iron losses account for only about 1-2mg per day [16] and therefore dietary uptake of iron only compensates for losses. Absorption can be regulated depending on iron need [17]. For example, during pregnancy or increased erythropoiesis, iron uptake is increased, whereas during iron overload, it is suppressed to maintain iron homeostasis [15]. Absorption of iron, both inorganic and heme-bound, occurs in the intestinal duodenum and is then transported to the blood plasma, where it is bound by transferrin (Tf). Only about 0.1% or 3mg of the iron in the body is bound by Tf [18]. Reticuloendothelial macrophages contain about 600mg of the metal, which is in a transit pool to the largest utilizer of the metal; the erythrocytes [13]. More than two thirds of the total body iron is present in hemoglobin within the erythroid compartment of the bone marrow and in mature circulating erythrocytes [19]. The rest of the iron in the body can be found within the liver, where about 1000mg is stored within ferritin, or in muscle and other tissues, accounting for 300mg of the metal [13].

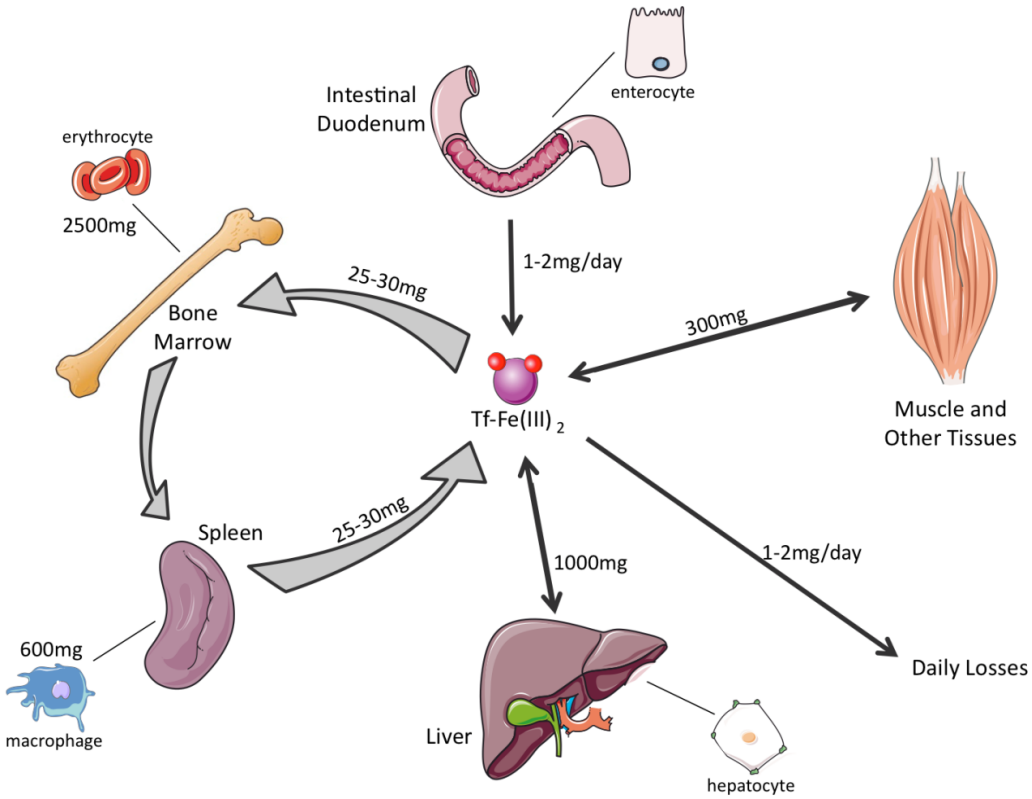

Figure 1.2: Iron distribution in the body. The 3-5 grams of body iron is distributed between developing erythrocytes in the bone marrow and circulating mature erythrocytes (2500mg), macrophages in the spleen that phagocytize senescent red blood cells (600mg), storage in the hepatocytes of the liver (1000mg), and muscles and other tissues (300mg). Enterocytes of the intestinal duodenum uptake 1-2mg/day of iron from the diet, which compensates for non-specific daily loses of the same amount. Iron is bound by transferrin (Tf) for the safe movement of plasma iron between the iron utilizing and iron storing tissues.

1.4 Iron Absorption into Enterocytes

Dietary iron uptake occurs in the enterocyte cells of the intestinal duodenum (Figure 1.3). Each individual cell has a microvillous brush border at its apical surface to increase the absorptive surface area [20]. Both forms of dietary iron, heme-bound and non-heme bound (inorganic), are absorbed at this surface but via different pathways.

1.4.1 Non-Heme Bound (Inorganic) Iron

Ferric iron is the main form of dietary inorganic iron, accounting for about 90% of nutritional intake but only 30% of absorbed iron due to low absorption efficiency [21]. Before it can cross the apical surface of the duodenal enterocyte, ferric iron must be reduced to ferrous iron by the membrane-associated ferrireductase duodenal cytochrome B (DcytB) [22]. Interestingly, DcytB knockout mice do not show an iron deficient phenotype as would be expected [23], indicating the possibility of other ferrireductase(s) on the apical membrane or the presence of dietary reducing agents [21]. Divalent metal transporter 1 (DMT1) transports the reduced ferrous iron across the apical membrane and into the cytoplasm of the enterocyte [24]. Unlike the $DcytB^{-/-}$ mouse, the DMT1 knockout mouse shows severe anemia owing to the essential role that DMT1 plays in intestinal iron absorption [25].

1.4.2 Heme Bound Iron

While heme-bound iron absorption across the apical enterocyte surface is known to be more efficient than inorganic iron absorption (40% and 5-10% respectively) [21], the mechanism of heme absorption is still poorly understood. Heme carrier protein 1 (HCP1), while predominantly being a folate transporter, is present on the apical surface of enterocytes and is proposed to be the protein involved in heme uptake into the cells [26]. It is believed that receptor-mediated endocytosis internalizes the heme, which is bound to HCP1 [27]. Then, heme can be either exported from the duodenal enterocytes intact via the feline leukemia virus, subgroup c, receptor (FLVCR) [28], or ferrous iron is released from it via heme oxygenase 1 (HO-1) [29] and the ferrous iron enters the same pathway as dietary inorganic iron for utilization within or export from the enterocyte.

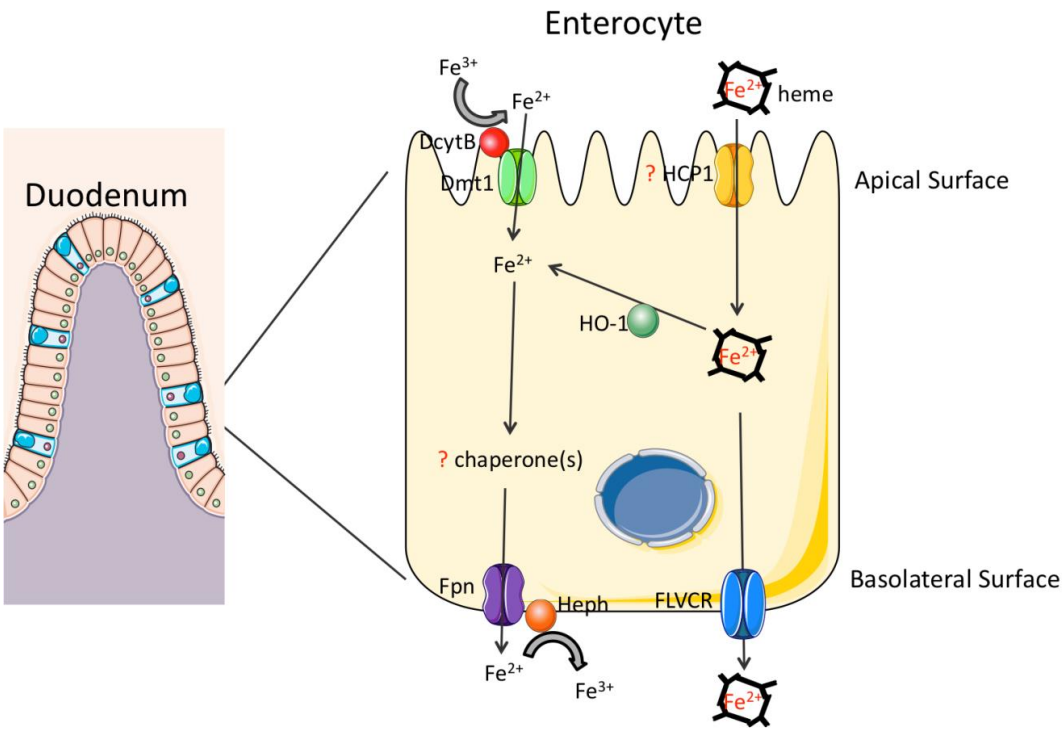

Figure 1.3: Dietary iron uptake by the enterocytes of the intestinal duodenum. Dietary iron is either in the form of non-heme bound (organic, ferric iron) or heme bound and each has a distinctive absorption pathway. Ferric iron is first reduced to ferrous iron at the apical membrane of the enterocyte by duodenal cytochrome B (DcytB) before divalent metal transporter 1 (DMT1) can transport it into the cytosol. Iron is exported at the basolateral surface via ferroportin (FPN) before being re-oxidized by hephaestin (Heph) to ferric iron for future binding to transferrin (Tf) in the plasma. Heme-bound iron is likely imported into the cytosol of enterocytes via heme carrier protein 1 (HCP1), where it can either be exported intact by the heme exporter feline leukemia virus, subgroup C, receptor (FLVCR), or degraded into ferrous iron by heme oxygenase 1 (HO-1). The ferrous iron then follows the same fate as the inorganic iron absorbed directly from the diet.

1.5 Iron Export to the Plasma

Intracellular iron trafficking from the apical surface to the basolateral membrane of the enterocyte is not yet fully understood (Figure 1.3). However, it is known that intracellular chaperones are involved and that the iron that enters the enterocyte has one of two possible destinations. A portion of the iron is utilized by the cell and owing to its short lifespan and subsequent sloughing, this iron is never absorbed into the body [20]. However, most of the iron that enters the enterocyte is exported to the plasma via the only known iron exporter: ferroportin (FPN) [30-32]. FPN knockout mice are embryonic lethal, whereas intestinal specific knockout mice confirm the necessity of FPN for iron absorption by the enterocytes [33]. FPN exports ferrous iron, which must be re-oxidized to ferric iron (for later binding to Tf) by the membrane bound intestinal ferroxidase hephaestin (Heph) [34]. Hephaestin not only oxidizes ferrous iron to ferric, but also maintains basolateral membrane localization of FPN [35], which helps to explain the hypochromic anemia and iron loading in the enterocytes of sla (Heph) mutant mice [34].

1.6 Transferrin Cycle

Iron absorbed through the duodenal enterocytes that is exported into the plasma is bound by Tf [36] (Figure 1.4). Tf is a powerful chelator that can tightly but reversibly bind two atoms of ferric iron [37]. Tf bound iron serves the purposes of maintaining the ferric iron in a soluble form at physiological pH 7.4 while keeping it in a redox-inert state to prevent the generation of toxic ROS, as well as facilitating iron transport and cellular uptake [13]. At this pH, iron loaded transferrin which is referred to as holo-transferrin, but not apo-transferrin which is transferrin not bound to iron atoms, binds with high affinity to the transferrin receptor 1 (TfR1) [38]. Cells that express TfR1, notably erythroid progenitor cells, hepatocytes, and rapidly dividing cell populations, can uptake the TfR1-$Tf(Fe)_2$ complex by receptor-mediated endocytosis [19]. The complex is rapidly internalized through clathrin-coated pits that become acidified to pH 5.5 by an ATP-dependent proton pump [17]. The acidic endosomal environment results in

a conformational change in both holo-transferrin and TfR1 which releases the ferric iron into the endosome [39]. The ferrireductase six transmembrane epithelial antigen of the prostate 3 (STEAP3) reduces the ferric iron to ferrous [40] such that DMT1 can transport the iron into the cytosol. The important role that DMT1 plays in this transferrin-mediated iron uptake cycle is highlighted by the severe iron-deficiency anemia phenotype that is coupled with liver iron acquisition in DMT1$^{-/-}$ mice [25]. The TfR1-Tf complex within the endosome is recycled to the cell surface, where at pH 7.4 in the plasma Tf dissociates from its receptor. It can now bind new ferric iron and repeat the cycle [38].

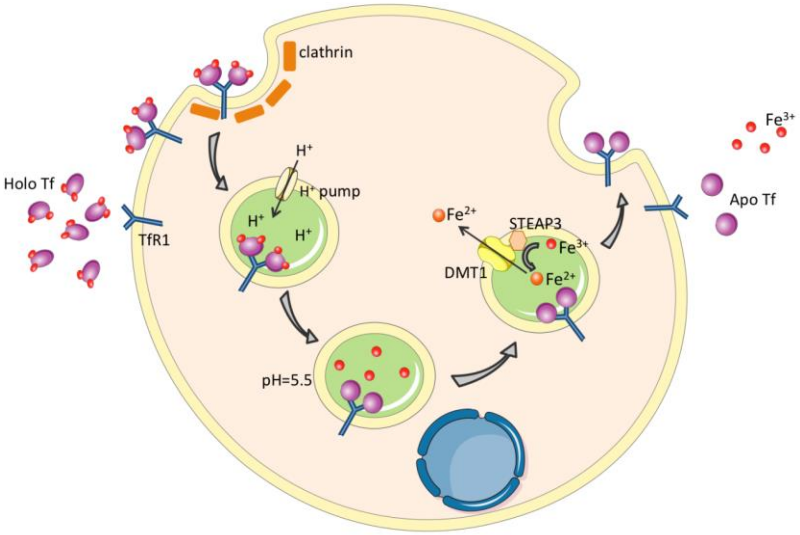

Figure 1.4: Transferrin mediated uptake of iron into cells. Each transferrin (Tf) can bind two atoms of ferric iron. Two iron loaded Tf, referred to as holo-transferrin, can bind the transferrin receptor 1 (TfR1) which undergoes rapid internalization into the cell via a clathrin coated pit. The resulting endosome becomes acidified by the action of an ATP-dependent pump. At pH 5.5, TfR1 and Tf undergo conformation changes, releasing ferric iron into the endosome. Six transmembrane epithelial antigen of the prostate 3 (STEAP3) reduces the iron to its ferrous form, which is exported into the cytosol by divalent metal transporter 1 (DMT1). Then the endosome is recycled to the cell membrane, where at physiological pH 7.4 iron replete Tf, referred to as apo-Tf, dissociates from TfR1 and begins again the cycle of binding ferric iron.

1.7 Tissue Iron Utilization

1.7.1 Erythrocytes

Tf is responsible in part for transporting and delivering iron to cells (Figure 1.2). A healthy individual will have transferrin saturation levels of approximately 30%. This leaves the remaining 70% of apo-transferrin to act as a buffering system for the plasma in order to prevent non-transferrin bound iron (NTBI) from accumulating and being deposited in tissue parenchymal cells to result in oxidative injury [41]. 80% of the diferric transferrin is shuttled to the erythroid progenitor cells [13] which have the highest iron demand. This is because these cells synthesize hemoglobin and therefore use two thirds of the body's iron which is found within heme [15]. For this reason, developing erythroid cells highly express TfR1 to uptake transferrin bound iron. Interestingly, immature erythroid cells can only uptake iron via the TfR1-$Tf(Fe)_2$ system whereas other cell types, including hepatocytes, are not strictly dependent on it [20]. This is highlighted by the embryonic lethality of TfR1 knockout mice and the severe microcytic hypochromic anemia and iron overload in non-hematopoietic cells in heterozygotes [42].

1.7.2 Macrophages

As mentioned, only 1-2mg per day of iron is absorbed from the diet, which results in the remaining 3-5 grams of body iron being continually recycled. This recycling occurs via the reticuloendothelial macrophages, primarily of the spleen, which phagocytize senescent erythrocytes [43]. The heme-bound iron is released by HO-1 and the ferrous iron is exported from the macrophages into the plasma via FPN and oxidized to ferric iron by the multi-copper containing ferroxidase ceruloplasmin (Cp) [44]. As seen in the sla mutant mouse, Cp knockout mice show anemia coupled with iron loading in macrophages and hepatocytes due to the impairment of iron efflux from the cells [44]. The ferric iron is bound by Tf in the same manner as the dietary iron that is absorbed through the duodenal enterocytes, however, macrophage iron recycling occurs to a much larger extent; at the rate of 25-30mg per day [17]. Since transferrin-bound iron only totals to

about 3mg, the rate of macrophage recycling of the metal means that the transferrin-bound iron turns over ten times per day [18]. This makes it the most dynamic iron pool in the body, moving between iron acquisition from the diet and macrophage recycling, delivery to erythroid precursor cells for utilization, and delivery to cells, primarily the hepatocytes of the liver, for storage.

1.8 Iron Storage

Cells possess the ability to store excess iron that is not in their immediate needs and therefore detoxify the cell by preventing 'free' iron from generating toxic ROS which result in OS damage [45]. This storage is performed in the cytosol by ferritin (Ft), a heteropolymer of heavy (H) and light (L) chains that form a hollow spherical shell [46]. 4500 ferric iron atoms, oxidized from the intracellular ferrous iron state by the ferroxidase activity of H-chain ferritin can be accommodated within a single Ft nanocage [47]. The ferroxidase activity is essential to the function of Ft since the H-chain knockout mouse is embryonic lethal [48]. When the cell later has iron-limiting conditions or the body needs iron for erythropoiesis, the metal can be released by the lysosomal and proteasomal degradation of Ft; thus releasing bioavailable iron for utilization [49]. This iron is transported to into the plasma in the same manner as the ferrous iron released from macrophages; via FPN and oxidized to ferric iron by Cp for binding to Tf. This storage process occurs primarily in the hepatocytes, since they are the body's main storage site for excess iron [50].

1.9 Systemic Iron Regulation

1.9.1 Hepcidin

Hepcidin (Hepc) was originally identified as an anti-microbial peptide [51], but is now known as the master regulator of systemic iron homeostasis. Hepatocytes produce the biologically active 25 amino acid peptide hormone, which is processed from the 84 amino acid preprohepcidin precursor by furin cleavage [52]. Despite other cell types that express Hepc, the main source of circulating Hepc is from the secretion of the peptide into the plasma from hepatocytes [53].

The inactivation of Hepc in mice results in a severe iron overload phenotype [54] while its overexpression has a severe iron deficiency anemia phenotype [55].

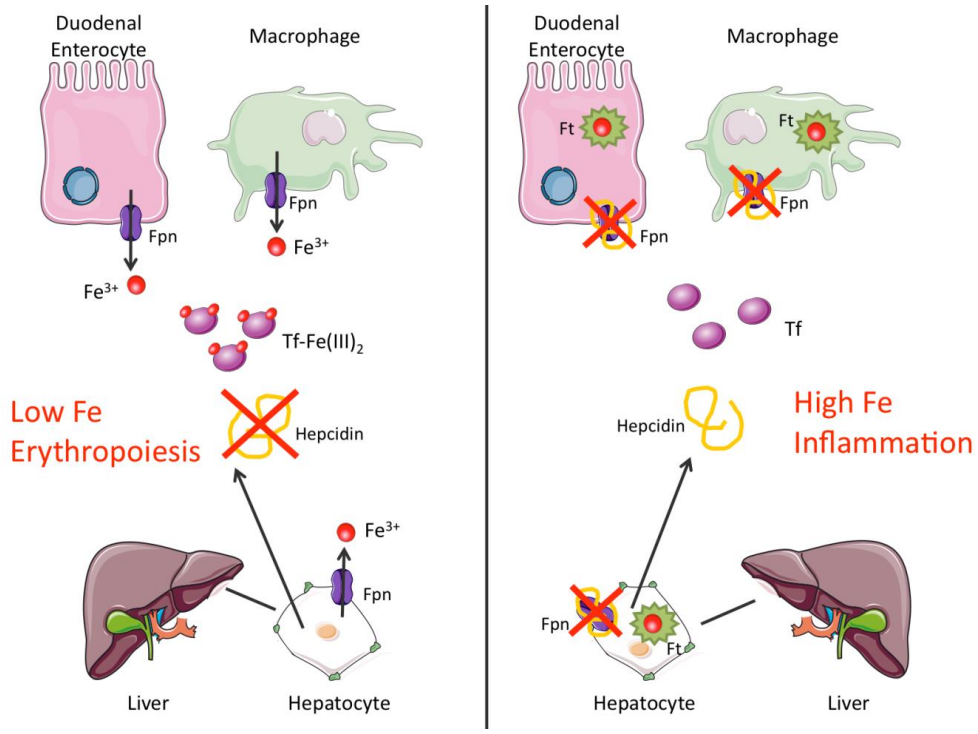

Figure 1.5: Systemic iron regulation is orchestrated by hepcidin. Hepcidin **(**Hepc) is a peptide hormone secreted into the plasma primarily from the hepatocytes. It can bind to ferroportin (FPN) expressed on the basolateral membrane of enterocytes, and the cell membrane of macrophages and hepatocytes. Upon binding, FPN is internalized, and undergoes ubiquitin dependent lysosomal degradation. Under low iron conditions or increased erythropoiesis, hepcidin is not produced by the liver (left). This results in iron release from the enterocytes uptaking dietary iron, from the macrophages recycling senescent red blood cells, and the hepatocytes storing iron in ferritin (Ft). This increases the pool of transferrin (Tf) bound ferric iron such that the body can now meet its iron needs. However, under high iron conditions or inflammation, Hepc is produced by the liver and binds to FPN (right). This results in a decrease in holo-transferrin and thus decreasing serum iron levels, as well as an increase in enterocyte, macrophage, and hepatocyte cellular iron, which is stored in Ft.

1.9.2 Hepcidin and Ferroportin

The absorption of dietary iron from the duodenal enterocytes, the release of recycled iron from macrophages, and the release of stored iron from hepatocytes is tightly controlled [53] (Figure 1.5). This is to maintain iron homeostasis, ensuring there is enough iron for erythroid cell development and cellular needs, but not more than. These cells all express FPN as their only iron exporter, which is where Hepc orchestrates the tight systemic control. Hepc directly binds to FPN and therefore negatively regulates iron efflux from these cells to the plasma [56]. Upon binding, FPN is internalized and undergoes ubiquitin dependent lysosomal degradation [56]. This results in cytosolic iron loading of enterocytes, macrophages, and hepatocytes, where the iron is stored in Ft, coupled with a decrease in Tf bound serum iron [17].

1.10 Hepcidin Regulation

Since Hepc orchestrates the tightly controlled systemic iron homeostasis, it too must be controlled to keep the iron balance (Figure 1.6). Firstly, this is achieved by being regulated by the object of its regulation; iron. Hepc is also regulated by erythropoiesis and inflammation [57].

1.10.1 Serum Iron

Hepc has been shown to respond to serum iron through changing Tf saturation levels. According to one proposed model, this pathway involves three proteins on the hepatocyte cell membrane: the hereditary hemochromatosis protein (HFE) and the transferrin receptors 1 and 2 (TfR1 and TfR2) as well as the circulating holo-transferrin [58, 59]. The holo-transferrin binding site on TfR1 is overlapping with the HFE binding site, resulting in only one of the two proteins being able to be bound to TfR1 at any given time [60]. Since holo-transferrin has a stronger binding affinity for TfR1 it will displace HFE when serum holo-transferrin concentrations are high [61]. This frees HFE for binding with TfR2 [62] and the complex is further stabilized by TfR2 binding to holo-transferrin [63]. Then this TfR2-HFE-$Tf(Fe)_2$ complex can induce Hepc expression by a signalling cascade

that possibly involves the bone morphogenetic protein (BMP)/ Homologs of both the *Drosophila* protein Mothers Against Decapentaplegic and the *C. elegans* protein SMA (SMAD) and/or the extracellular signal regulated kinase 1/2 (ERK 1/2) and mitogen-activated protein kinases (MAPK) pathways [64-66]. The overall outcome of this cascade is an increase in Hepc which reduces serum iron concentrations by eliminating iron efflux from FPN expressing cells (enterocytes, macrophages, and hepatocytes).

1.10.2 Hepatic Iron

There are several proteins that are involved in hepatic iron signalling to Hepc, of which the BMP/SMAD pathway is critical. It begins with BMP6 expression in the liver being upregulated in response to increasing hepatic iron stores [67]. BMP6 is then secreted to the plasma where it binds its BMP receptor (BMPR) [68]. Hemojuvelin (HJV) acts as a co-receptor on the plasma membrane of hepatocytes to enhance the SMAD signalling cascade [69]. SMAD 1/5/8 is phosphorylated which results in recruitment of SMAD4 and translocation of the complex to the nucleus [67]. The complex can then bind to proximal and distal sites of the Hepc promoter to activate its expression [70]. There are also BMP responsive elements in the Hepc promoter, however it is unclear how they regulate Hepc expression [71]. The pathway is further controlled via the upstream transmembrane serine protease 6 (TMPRSS6), also known as Matriptase-2, which cleaves HJV from the membrane and therefore attenuates Hepc induction [72]. This BMP/SMAD pathway is the most powerful known mechanism in the transcriptional regulation of Hepc [20] and the possibility of there being crosstalk between the hepatic and serum iron sensing pathways cannot be ignored. The power of this signalling cascade is highlighted by the phenotype of $BMP6^{-/-}$, hepatocyte-specific $SMAD4^{-/-}$, or $HJV^{-/-}$ mice which all display markedly reduced hepcidin expression and massive iron overload [73-75].

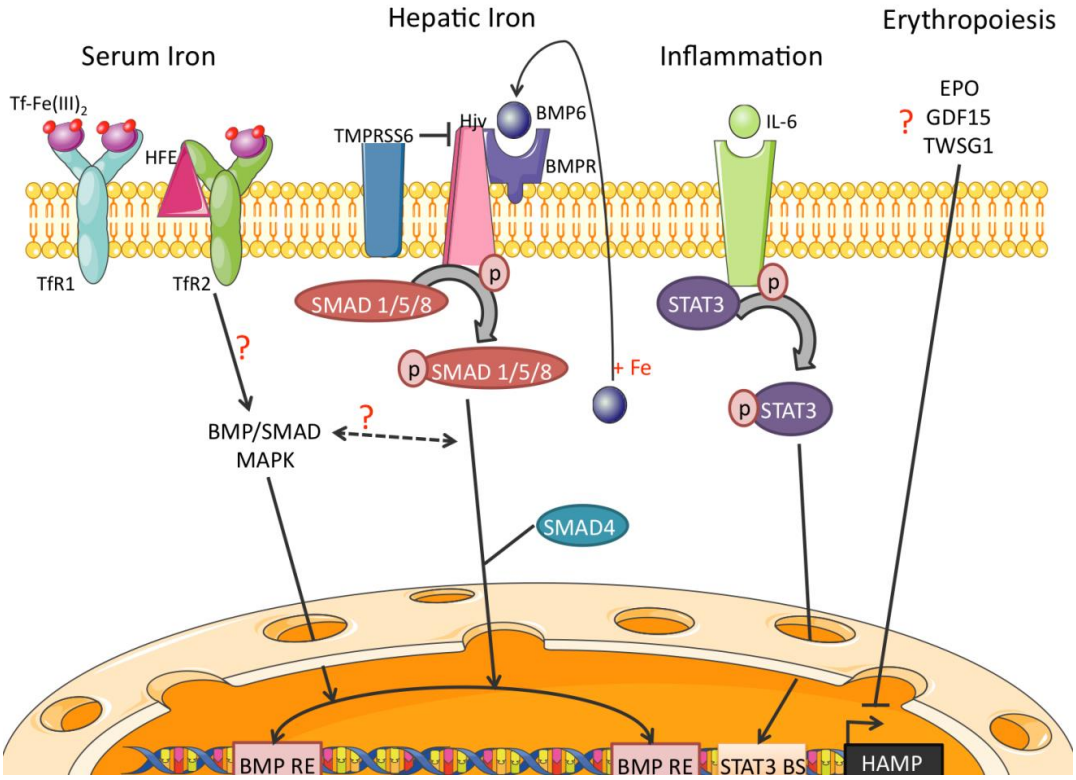

Figure 1.6: Hepcidin regulation from iron, inflammatory, and erythropoiesis cues. Hepcidin (Hepc) is regulated by two forms of body iron. Serum iron levels are sensed by the human hemochromatosis protein (HFE), transferrin receptor 1 (TfR1), transferrin receptor 2 (TfR2), and holo-transferrin. Under high iron conditions, holo-transferrin binds to TfR1 displacing HFE for binding to TfR2. This TfR2/HFE complex, along with holo-transferrin, can then signal Hepc transcription possibly via the bone morphogenetic protein (BMP)/ Homologs of both the *Drosophila* protein Mothers Against Decapentaplegic and the *C. elegans* protein SMA (SMAD) and/or the extracellular signal regulated kinase 1/2 (ERK 1/2) and mitogen-activated protein kinases (MAPK) pathways. Hepatic iron levels are sensed by BMP6, bone morphogenetic protein receptor (BMPR), and hemojuvelin (HJV). This generates a signalling cascade with phosphorylated SMAD 1/5/8 and SMAD4 complexing, translocating to the nucleus, and binding to sites in the promoter to induce Hepc expression. Inflammation is sensed primarily by the cytokine interleukin-6 (IL-6). Upon binding to its receptor, IL-6 promotes phosphorylation of signal transducer and activator of transcription 3

(STAT3), which translocates to the nucleus and binds to the Hepc promoter. Erythropoiesis sensing is less understood, but is thought to involve erythropoietin (EPO), growth differentiation factor 15 (GDF15), and twisted gastrulation homologue 1 (TWSG1) which suppress Hepc expression.

1.10.3 Inflammation

Besides iron-induced expression of Hepc, inflammatory signals also increase Hepc expression as well. In hepatocytes, this increase is mediated primarily by the pro-inflammatory cytokine interleukin-6 (IL-6) [76]. IL-6 exerts its control via a signalling cascade where signal transducer and activator of transcription 3 (STAT3) becomes phosphorylated, translocates to the nucleus, and binds to a STAT3 consensus site in the Hepc promoter [77].

1.10.4 Erythropoiesis

Since the largest consumer of iron in the body are the erythroid cells, it is logical that Hepc expression is controlled by erythropoiesis cues. These cues have a greater influence over Hepc expression than does iron status [57], however the origin of the signal, likely molecules released from erythroid precursors, is not fully understood [50]. Three candidates that all suppress Hepc expression are growth differentiation factor 15 (GDF15), twisted gastrulation homologue 1 (TWSG1) and erythropoietin (EPO) [78-80]. This suppression in Hepc results in more iron being available for erythropoiesis since FPN is not degraded and therefore can export iron from the dietary uptake, recycling, and storage.

1.11 Iron Misregulation

Despite the tight regulation of systemic iron levels, there are many diseases associated with aberrant iron homeostasis. Diseases can either cause iron overload or deficiency and most often are the result of a genetic mutation.

1.11.1 Iron Overload – Hereditary Hemochromatosis

Hereditary hemochromatosis (HH) is caused by autosomal recessive mutations in different genes in the Hepc regulatory pathways which results in inadequately low levels of Hepc expression when compared to body iron loading [81]. This results in hyperabsorption of dietary iron, increased NTBI, and parenchymal tissue loading leading to iron-induced tissue damage [17]. There are four types of HH with all except type IVb being characterized with elevated Tf saturation, elevated serum Ft, and tissue iron overload of the liver, heart, pancreas, and skin [50]. This loading may lead to liver fibrosis and cirrhosis, heart failure, diabetes, cardiomyopathy, and pigmentation of the skin [81]. The most frequent form of HH, Type I, arises from a homozygous missense mutation in the *HFE* gene. The common C282Y mutation leads to a misfolding of HFE due to the lack of a disulfide bridge, such that it does not localize to the plasma membrane [82]. The lack of functional HFE results in a blunted Hepc response to body iron levels. HH Type II is a result of mutations in either *HJV* or *HAMP* (the gene that encodes Hepc) genes [83, 84]. Type II presents with more severe iron loading and an earlier onset than Type I, and hence is known as juvenile hereditary hemochromatosis [84]. The result of the mutations in either gene is almost undetectable levels of Hepc in the plasma despite massive hepatic iron loading [83]. HH Type III is caused by a rare autosomal recessive mutation in the *TfR2* gene and presents with an intermediate phenotype between Types I and II [85]. Interestingly, combined *HFE* and *TfR2* mutations are phenotypically identical to juvenile HH [86]. HH Type IV is due to mutations in FPN, and therefore is also called ferroportin disease [87]. Unlike the other types of HH, Type IV is not due to the impairment of Hepc production. Mutations in FPN that result in Hepc failing to properly bind it or in impairment of bound FPN-Hepc internalization and degradation generate the HH phenotype of high Tf saturation and hepatocyte iron loading [88-90]. However, other mutations in FPN resulting in reduced membrane localization or impaired iron transport causes HH type IVb and has the opposite phenotype; low serum iron and macrophage iron accumulation [88-90].

Disease	Cause	Phenotype
HH Type I	*HFE* gene mutation	↓ Hepc ↑ Iron loading
HH Type IIA	*HJV* gene mutation	↓↓↓ Hepc ↑↑↑ Iron loading
HH Type IIB	*HAMP* gene mutation	↓↓↓ Hepc ↑↑↑ Iron loading
HH Type III	*TfR2* gene mutation	↓↓ Hepc ↑↑ Iron loading
HH Type IVa	FPN protein mutation	Normal Hepc ↑ Hepatic and Tf-bound iron
HH Type IVb	FPN protein mutation	Normal Hepc ↓ Hepatic and Tf-bond iron ↑ Macrophage iron loading
ACD	Infection, inflammation	↑ Hepc ↓ Iron loading
IRIDA	*TMPRSS6* gene mutation	Normal or ↑ Hepc ↓ Iron loading

Table 1.1: Iron misregulation resulting in iron overload (hereditary hemochromatosis (HH)) or iron deficiency (anemia).

1.11.2 Iron Deficiency – Anemias

Blood loss, insufficient iron uptake, or overexpression of Hepc leads to anemia that most often presents as microcytic anemia. Like HH, anemia can be caused by a genetic mutation in dietary iron uptake genes or can be acquired, and is characterized by an increase in Hepc expression and decreased serum iron levels [15]. Anemia of chronic diseases (ACD) is an acquired form of anemia seen in patients with trauma, infections, and chronic inflammation from a variety of diseases [91]. Hepc is activated by elevated levels of inflammatory cytokines, especially IL-6, which causes hypoferremia [92]. The resulting low serum iron

levels could be a mechanism to limit bacteria growth during an infection by limiting their supply of iron [93]. However, if the inflammation or infection persists, then erythropoiesis is compromised resulting in decreased life span of red blood cells [91]. Iron-refractory iron deficiency anemia (IRIDA) is a genetic disorder caused by an autosomal recessive mutation in *TMPRSS6*, which is a negative regulator of Hepc expression [94]. Despite severe iron deficiency, Hepc expression is normal or upregulated and is not depressed with oral iron administration [94].

CHAPTER 2

Iron regulation of SERPIN B3 mRNA *in vitro* and its function in iron homeostasis

2.1 PREFACE

Rational of the study:

SERPIN B3 mRNA was seen to be overexpressed in the livers of Hjv-/- mice, which exhibit severe hepatic iron overload. SERPIN B3 mRNA expression also positively correlated with dietary iron challenge in wild type mice.

The direct or indirect effect of iron on the expression of SERPIN B3 mRNA had not yet been elucidated and was investigated here.

Also, the possible function of SERPIN B3 in iron homeostasis, owing to its overexpression in the specific mouse model was investigated.

2.2 ABSTRACT

SERPIN B3 (SB3) formally known as Squamous Cell Carcinoma Antigen 1 (SCCA1) is a member of the ov-serpin family of serine protease inhibitors. It is expressed at low levels in normal epithelial cells of the esophagus, cervix, upper airways, and skin but is overexpressed in squamous cell carcinomas in the lungs, head and neck, and cervix as well as in hepatocellular carcinomas and damaged hepatocytes. Known activators of SB3 include radiation and IL-6; the latter triggers phosphorylation of STAT-3, which binds to the SB3 promoter resulting in inhibition of apoptosis and increased cell survival. It was observed that SB3 mRNA was highly expressed in the livers of hemojuvelin (HJV) knockout mice, a model of hereditary iron overload (hemochromatosis). Furthermore, SB3 mRNA expression was positively regulated by dietary iron in wild type mice. Therefore, the possible regulation of SB3 mRNA at the transcriptional level was investigated by developing indicator constructs of the SB3 promoter fused to the *luciferase* gene. By transient transfection assays, it was determined that the promoter exhibits weak activity in the human hepatoma cell line Huh7. With the addition of iron sources or an iron chelator overnight, there was no difference in promoter activity, nor were there differences with six-hour treatments with mild oxidative stress inducing agents. Endogenous levels of SB3 mRNA were determined using qPCR after the same iron and chelator treatments. Huh7 cells showed no expression of SB3 mRNA, whereas HA22T/VGH cells, a liver endothelial cell line, and HeLa cells showed only mild induction with hemin iron treatments. Thus, SB3 mRNA transcription is not regulated by iron *in vitro* and we conclude that the robust iron-dependent regulation of SB3 in the mouse liver is not caused by cell autonomous transcriptional regulation. The function of SB3 has not been investigated in iron homeostasis, however its overexpression in the $HJV^{-/-}$ mouse leads to the hypothesis that it may act upstream of hepcidin in the TMPRSS6/HJV/BMP6 pathway. It is likely that SB3 likely does not directly act on TMPRSS6 owing to the fact that SB3 selectively inhibits papain-like cysteine proteases unlike TMPRSS6 which is a serine protease. However, further investigations into the function of SB3 need to be performed.

2.3 INTRODUCTION

The serine protease inhibitor, clade B3 (SERPIN B3 or SB3), formally known as squamous cell carcinoma antigen 1 (SCCA1), belongs to a large family of serine protease inhibitors called serpins [95]. Serpins, as their name suggests, are protease inhibitors but also perform a number of other biological tasks not relating to this ability. Of the 37 serpins identified in humans, only 26 are inhibitory [96]. The remaining 9 are implicated in hormone transport, blood pressure regulation, and neurological development [96, 97]. While serpins share a conserved tertiary structure, it is the reactive center loop (RCL) that gives each serpin its specificity in its inhibitory function [95]. The RCL is approximately 17 amino acids long and matches the amino acid sequence of the protease active site [98]. The target protease binds the serpin by its RCL which results in a conformational change in the serpin from its native stressed form to its bound relaxed one [99]. Then the protease cleaves the serpin at the scissile bond between residues P1-P1' causing an irreversible conformational change in the serpin [100]. For this reason, the serpin exhibits its inhibitory function via a 'suicide mechanism'. The serpin is inactivated by the cleavage but so too is the protease since it becomes irreversibly covalently bound to the serpin [101]. While the exact mechanism that SB3 uses to inhibit its target proteases is not fully understood it is known that SB3 does not covalently bind to the protease. Instead it blunts the protease's function via inducing a conformational change in the protease and itself [102].

Within the superfamily of serpins there are 9 groups, or clades, in humans [95]. Serpins are sorted into clades by the conservation of amino acid sequence and therefore by common functionality [103]. Clade B serpins are termed ovoalbumin serpins (ov-serpins) and there are 13 members in the group with conserved amino acid sequence (38-50%), a common structure, and a lack of a signal sequence [104]. This lack of an N-terminal signal sequence required by the secretion pathway ensures that clade B serpins remain intracellularly within the cytosol [95]. All other serpins are excreted and therefore are found extracellularly. These intracellular ov-serpins not only inhibit proteases, but also regulate apoptosis,

inflammation, and tumor growth, therefore exerting a cytoprotective function for the cell [96].

SB3 was first isolated from squamous cell carcinoma of the uterine cervix, and hence its original name of SCCA1 [105]. It is now known to be expressed by healthy epithelial cells of the esophagus, cervix, upper airways, thymus, and skin but its expression is elevated in squamous cell carcinomas (SCC) in the lungs, head and neck, and cervix [106]. For this reason, SB3 is used as a marker of SCC since it is passively released by these cancer cells into the serum [107]. Recently, it has been reported that SB3 is overexpressed in liver carcinomas, specifically hepatocellular carcinoma (HCC), and is produced by damaged hepatocytes [108, 109]. SB3 along with the other ov-serpins is a known regulator of apoptosis, and therefore its overexpression in cancer cells may prolong their lifespan. By inhibiting apoptosis in cancer cells, SB3 rescues the cells from death and therefore attributes to the decreased prognosis for the patients with these cancers [96]. The role of SB3 in apoptosis is thought to be upstream of caspase-3, interfering with cytochrome C release from the mitochondria [110] by inhibiting papain-like cysteine proteases [111]. There is however the possibility of mechanistic overlap such that SB3 can inhibit serine proteases as well like the other members of its serpin family.

Known activators of SB3 are radiation, IL-6 (interleukin-6), and TNFα (tumour necrosis factor α), which are all implicated in apoptosis pathways. UV radiation is known to activate p38 MAPK (mitogen activated protein kinase), JNK1 (c-Jun NH_2-terminal kinase 1), and therefore caspase 3 and 9 [112]. In cells overexpressing SB3, UV dependent phosphorylation of p38 MAPK was decreased and so too was the presence of activated caspase-9 and therefore downstream caspase-3 activity [113]. SB3 also suppresses the kinase activity of JKN1 upon UV radiation [114]. IL-6 is known to trigger the phosphorylation of STAT-3 (signal transducer and activator of transcription 3), which can translocate to the nucleus and bind to consensus sites in the promoter of a target genes to

induce its expression [115]. This occurs with SB3, since pSTAT-3 binds to its promoter and therefore activates SB3 gene expression [116]. TNFα is known to induce apoptosis by the caspase-3 pathway as well. Interestingly, TNFα also positively regulates the expression of SB3, which downregulates caspase-3 [117]. The end result of all of these activators of SB3 is a decrease in the apoptosis pathways and an increase in cell survival.

In a collaborative study between the laboratories of Drs Pantopoulos and Pontisso, another possible regulator of SB3 was found. The phenotype of HJV (hemojuvelin) knockout mice, a mouse model of HH (hereditary hemochromatosis), is profound iron overload of the liver and very low levels of hepcidin (Hepc) expression, the hormone peptide orchestrating systemic iron control [75]. There is already an established link between iron loading and damage to hepatocytes and the liver [15], which can predispose humans to cirrhosis, fibrosis, and HCC. However, mouse models are spared from liver damage even in the presence of elevated hepatic iron loading, but $HJV^{-/-}$ mice are sensitized to chemical induced liver fibrogenesis and do develop liver diseases [118]. SB3 is a marker of liver disease and its expression is increased in both HCC and damaged hepatocytes [108, 109]. Therefore the $HJV^{-/-}$ livers, showing massive iron loading and damage were investigated for SB3 expression. It was observed that SB3 mRNA was highly expressed in the livers of these mice as compared to WT (wild type) mice (Figure 2.1A). Next, it was found that SB3 mRNA expression in the livers of the $HJV^{-/-}$ mice was significantly increased with the administration of dietary iron. Furthermore, it was observed that mRNA expression was positively regulated by the dietary iron challenge in the WT mice as well (Figure 2.1B). This positive effect of iron on SB3 mRNA expression was maintained at the protein level with immunohistochemistry showing a marked rise in SB3 protein expression in $HJV^{-/-}$ livers from mice challenged with high iron (Figure 2.1C).

Since the above *in vivo* data demonstrated a positive link between SB3 expression and liver iron loading in $HJV^{-/-}$ mice, we hypothesized that a) SB3 is regulated transcriptionally by iron, and b) SB3 may be involved in the regulation of Hepc. It is known that Hepc is induced by hepatic iron stores via bone morphogenetic protein 6 (BMP6), HJV, and a homologs of both the *Drosophila* protein, Mothers Against Decapentaplegic and the *C. elegans* protein SMA (SMAD) signaling cascade [67-71, 73]. This pathway is subject to further control via the transmembrane serine protease 6 (TMPRSS6), also known as matriptase-2. TMPRSS6 cleaves HJV from the membrane, therefore attenuating its signaling to Hepc [72]. Since SB3 could have mechanistic overlap to inhibit serine proteases, as well as its well-established inhibition of papain-like cysteine proteases [111], we investigated its potential upstream role on TMPRSS6 in this Hepc expression pathway.

2.4 MATERIALS AND METHODS

2.4.1 Plasmid Construction

SERPIN B3 (SB3) promoter: Whole human genomic DNA was extracted from the human renal carcinoma 786O cells and used as a template for PCR amplification. Phusion High-Fidelity DNA Polymerase (Finnzymes) and primers as in Table 2.1 were cycled as follows: initial denaturation 98°C 30sec, 36 cycles of 98°C 10sec, 68°C 30sec, 72°C 3mins, and final extension 72°C 10mins. PCR products were run on a 1% agarose-TBE gel to confirm correct size, excised, and gel purified (QIAquick Gel Extraction, Qiagen). The pGL3 basic vector (Promega) containing the firefly luciferase (*luc*) reporter gene and appropriate PCR products were digested for 2.5hrs with restriction enzymes BglII and MluI (NEB) at 37°C and the vector was further incubated with calf intestinal phosphatase (CIP) (NEB) for 45mins at 37°C. Ligations were performed with T4 Ligase (NEB) on the digested and gel purified PCR products and vector overnight at room temperature before transformation into NEB10β competent cells (NEB). Maxiprep on

confirmed colonies (ENZA FastFilter DNA, Omega Bio-Tek) were performed and plasmids were sequenced (McGill University and Genome Quebec Innovation Center) to verify correct orientation upstream of the *luc* gene.

2.7Kb Hepc-pGL3 basic: The 2.7Kb Hepc-pGL3 plasmid, containing 2.7Kb of the hepcidin promoter cloned into the pGL3 basic vector, was kindly provided by Dr. M. Muckenthaler [119].

pRL-TK, GFP, pBABEpuro: the pRL-TK plasmid, containing the renilla (*ren)* luciferase reporter gene used as a transfection control was purchased from Promega. The GFP mammalian expression plasmid was purchased from Lonza and the pBABEpuro plasmid expressing the puromycin (puro) gene was a gift from Dr. F.A. Mallette [120].

HJV WT-pTRE2hyg2-Myc and G320V-pTRE2hyg2-Myc: HJV WT-HA-pUHD10.3 and HJV G320V-HA-pUHD10.3 cDNA in the tet-inducible promoter pUHD10.3 vector were generated previously in the lab with the HJV cDNA that was kindly provided by Dr. P. Goldberg (Xenon Pharmaceuticals). These plasmids were used as templates for PCR amplification as per SB3 promoter protocol, with the following modifications. PCR cycling condition: initial denaturation 98°C 30sec, 10 cycles of 98°C 10sec, 62°C 30sec, 72°C 1min, 25 cycles of 98°C 10sec, 72°C 1min, and final extension 72°C 10mins. The pTRE2hyg2-Myc vector (Clontech) containing both a tet-inducible promoter and hygromycin (hyg) resistance gene and appropriate PCR products were digested with restriction enzymes NotI and MluI (NEB) at 37°C. Plasmids were sequenced (McGill University and Genome Quebec Innovation Center) to verify correct orientation and fusion to the N-terminal Myc tag.

SERPIN B3 WT-V5 and SERPIN B3 dHinge-V5 cDNA: SB3 WT cDNA in the pcDNA3.1 V5 His TOPO vector (Invitrogen) [109] and SB3 dHinge-V5 cDNA in the pcDNA3.1 V5 His vector (Invitrogen) [121] and were kindly provided by Dr. P. Pontisso. The B3 WT plasmid was used as a template for PCR amplification as per SB3 promoter protocol with the following modifications. PCR cycling conditions: initial denaturation 98°C 30sec, 36 cycles of 98°C 10sec, 72°C 1min, and final extension 72°C 10mins. The SB3 dHinge-pcDNA3.1 V5 His vector and

the appropriate PCR product were digested for 2.5hrs with restriction enzyme XhoI (NEB) at 37°C and a further 2.5hrs with BstBI (NEB) at 65°C. The plasmid was sequenced (McGill University and Genome Quebec Innovation Center) to verify correct orientation upstream and fusion to the C-terminal V5 tag.

TMPRSS6 WT-FLAG and TMPRSS6 MASK-FLAG cDNA: TMPRSS6 WT-FLAG in the pcDNA3.1 vector (Invitrogen) [122] and TMPRSS6 MASK-FLAG in the pcDNA3.1 vector (Invitrogen) [72] were kindly provided by Dr. C. Camaschella.

SB3 promoter 5Kb - F	TGTACGCGTGTGAATATGAAGGAGCAG
SB3 promoter 4Kb - F	ACTACGCGTGATGGGACTTTCCTCATC
SB3 promoter 3Kb - F	ACGACGCGTGAAATGCCAAGATACATAAG
SB3 promoter 2Kb - F	GATACGCGTAACAAACTCATGGCTGGTG
SB3 promoter 1Kb - F	ACCACGCGTGAGATTAGGAAGTAAAAGAGG
SB3 promoter .5Kb - F	AGCACGCGTTTGGACTTAGAATTAGCACTA
SB3 promoter - R	GCGAGATCTGTGGAATGAAGGGTGAGA
HJV WT/G320V - F	CTAGACGCGTCCATGGGGGAGCCAGGCCAGTC
HJV WT/G320V - R	CCTTGCGGCCGCTTACTGAATGCAAAGCCACA
SERPIN B3 WT - F	CTCGCTCGAGATGAATTCACTCAGT GAAGC
SERPIN B3 WT - R	TCTAAGTTCGAACGGGGATGAGAATCTGCCAT

Table 2.1: Primer sequences for plasmid construction. Restriction enzyme sequences are underlined.

2.4.2 Cell Culture

Huh7, a human hepatoma cell line, and HA22T/VGH, a liver endothelial cell line, were maintained in Dulbecco's Modified Eagle's Medium 1x (DMEM) with 4.5g/L glucose, L-glutamine, and sodium pyruvate supplemented with 10% FBS, 1x penicillin/streptomycin (PS), and 1x non-essential amino acids (all from WISENT) in a humidified incubator at 37°C with 5% CO_2. HeLa cells were cultured in the same manner, excluding 1x non-essential amino acids. For tet-

inducible stable clone analysis, Huh7-tTA cells were grown in DMEM supplemented with 10% tetracycline-free FBS (Clontech), 1x PS, 1x non-essential amino acids, and 250µg/mL G418 (WISENT). H1299, a non-small cell lung carcinoma cell line, stabily expressing HJV WT or G320V mutant cDNA used for tet-inducible stable clone analysis were grown as Huh7-tTA cells except with the addition of 2µg/mL puromycin (Sigma).

2.4.3 Cell Culture Treatments

Iron treatments: Cells were treated overnight with either 50µM hemin (Sigma), 3µg/mL fresh ferric ammonium citrate (FAC) (Sigma), or 100µM deferoxamine (DFO) (pharma science).

IL-6 treatments: Cells were treated overnight with 5ng/mL human recombinant IL-6 (Sigma).

Antibiotics: Cells were treated with 250µg/mL G418 (WISENT) or 2µg/mL puromycin (puro) (Sigma).

Tetracycline: Cells were treated with or without 2µg/mL tetracycline (tet) (Fisher Biotech).

Oxidative stress: Cells were treated with glucose oxidase (GOx) (Sigma), menadione (Sigma), hydrogen peroxide (H_2O_2) (Sigma), or cobalt chloride ($CoCl_2$) (Fisher Biotech) at the indicated concentrations for 6hrs. Production of H_2O_2 was monitored with Quantofix Peroxide 25 semi-quantitative test strips (Sigma).

2.4.4 Luciferase Assay

Huh7 or HeLa cells were seeded at a density of $7.5*10^4$ cells/mL or $1.5*10^5$ cells/mL respectively in a 12 well dish in media lacking antibiotics and incubated overnight. Transient transfections were performed the next day using Lipofectamine2000 (Invitrogen) as per the manufacturer's protocol for a 24 well dish. 0.5µg of the pGL3-promoter constructs as well as 0.3µg of the pRL-TK plasmid were diluted in 50µL of 1x OPTI-MEM reduced serum media (WISENT) and 2µL of Lipofectamine2000 was diluted in a further 50µL of OPTI –MEM for

5 mins. Plasmids and Lipofectamine2000 were combined and incubated at room temperature for 20 minutes before plating with cells in their overnight growth media for 4hrs at 37°C. Cells were then washed once with regular media, and incubated for 48hrs in fresh regular media. Cells were lysed in 250µL 1x Passive Lysis Buffer (Promega) on a rocker at room temperature for 20 mins and luminescence from *luciferase* was measured and standardized to *renilla* luminescence using the Dual Luciferase Reporter Assay (Promega). Values are reported as percentages of *luc* activity.

2.4.5 qPCR

Total RNA was extracted with TRIzol (Invitrogen) from cell pellets washed and collected via scraping in sterile cold 1x PBS as per the manufacturer's protocol. cDNA was synthesized from 1µg of RNA with the QuantiTect Reverse Transcription kit (Qiagen) as per the manufacturer's protocol. SYBR Green (Qiagen) and gene specific primers in Table 2.2 were used to amplify products with the following cycling conditions: initial denaturation 95°C 15mins, 40 cycles of 95°C 15sec, 55°C 45sec, 72°C 30sec, and final cycle melt analysis from 55°C to 95°C for qPCR analysis. Data was normalized to GAPDH reference gene and reported as fold increases.

SERPIN B3 - F	GCAAATGCTCCAGAAGAAAG
SERPIN B3 - R	CACTGCCCTTTGAAATAGATTG
GAPDH - F	TGGTATCGTGGAAGGACTCATGAC
GAPDH - R	ATGCCAGTGAGCTTCCCGTTCAGC

Table 2.2: Primer sequences for qPCR

2.4.6 Stable Clones

Transfections following the manufacturer's protocol using 60µL of Lipofectamine2000 with 21.6µg of HJV WT-HA-pUHD10.3 or G320V-HA-

pUHD10.3 plasmids being co-transfected with 2.4µg of pBABEpuro into Huh7 tTA cells (a kind gift of Dr. M. Nassal [123]) were performed. Cells were maintained in regular media with 250µg/mL G418 and were selected for puro resistance 3 days post transfection. Positive clones were grown for 72hrs in tet-free media, supplemented with or without 2µg/mL tet for tet inducability analysis.

2.4.7 Western Blots

Cells were collected via washing and scraping in 1x cold sterile PBS. Protein was extracted on ice for 45mins using RIPA (50mM Tris-HCL pH 7.5, 150mM NaCl, 0.1% SDS, 0.5% sodium deoxycholate, and 1% Triton X-100) and boiled at 95°C for 5mins in sample buffer (62.5mM Tris-HCL pH 6.8, 50% glycerol, 2% SDS, and 50mM DTT). 10-15% SDS-PAGE gels were used to separate proteins, which were transferred onto nitrocellulose membranes (BioRad) and blocked in 5% milk TBS-T (Tris Buffered Saline – tween 20) for 1hr at room temperature. Membranes were probed overnight at 4°C with primary antibodies β-actin (Sigma), HJV #24 (generated in-lab), HO-1 (Enzo), Ferritin (Novus Biologicals), or Myc (Santa Cruz Biotechnology) at 1:1000x, V5 (Invitrogen) at 1:2000x, or FLAG (Sigma) at 1:500x dilutions in 5% milk TBS-T. Membranes were washed for 3 x 10mins with fresh TBS-T and incubated with appropriate HRP conjugated secondary antibodies diluted in 5% milk TBS-T for one hour at room temperature. Membranes were washed again for 3 x 10mins with fresh TBS-T and detection of peroxidase-coupled antibodies was performed with the enhanced chemiluminescence method (Perkin-Elmer) onto X-ray film (UniDent Scientific).

2.4.8 Statistical Analysis

Data is expressed as mean ± standard error mean (SEM). Analysis of multiple groups was performed with 1-way ANOVA in the Prism GraphPad software (version 5.0d). A probability value of $p < 0.05$ was considered to be statistically significant.

2.5 RESULTS

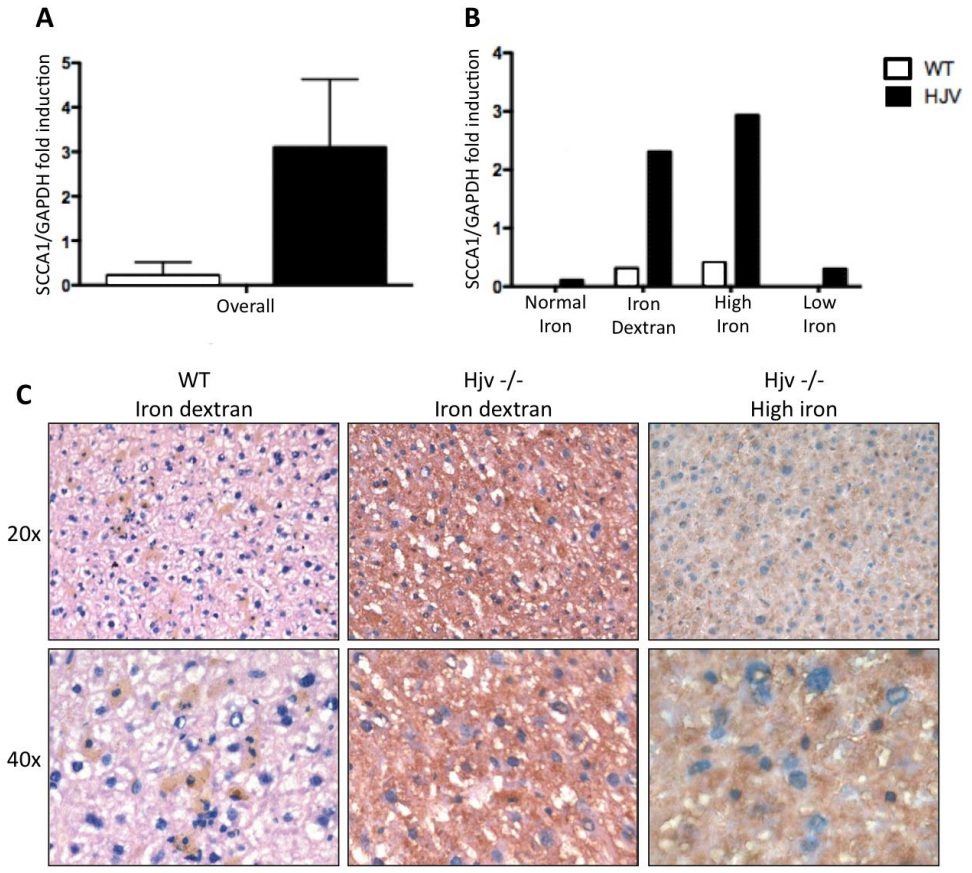

Figure 2.1: SERPIN B3 is overexpressed in the livers of hemochromatotic mice and is regulated by dietary iron. All data was performed by Dr. Pontisso's laboratory. (A) SB3, formally known as SCCA1, mRNA expression in hemojuvelin (HJV) knockout mice (black bar) as compared to wildtype (WT) mice (white bar) on a standard diet is significantly increased 15-fold ($p<0.001$). (B) When $HJV^{-/-}$ mice were challenged with iron dextran, SB3 mRNA expression was significantly increased 7.5-fold as compared to WT mice ($p<0.05$) and significantly increased 18-fold as compared to normal diet $HJV^{-/-}$ mice ($p<0.01$). For $HJV^{-/-}$ mice challenged orally with iron via carbonyl iron in the chow (high iron), SB3 mRNA expression was significantly increased as compared to both WT mice (6-fold) and normal diet $HJV^{-/-}$ mice (20-fold) (both $p<0.001$). (C) Immunohistochemistry of SB3 expression in the liver of WT and $HJV^{-/-}$ mice challenged with iron show a significant increase of SB3 protein in only the livers of the $HJV^{-/-}$ mice.

2.5.1 SERPIN B3 promoter shows weak activity *in vitro*

Expression vectors for the human promoter of SB3 were generated by cloning up to 5Kb upstream of the transcription start site into the promoterless pGL3 basic vector. Truncated promoter fragments with deletions of 1Kb each, as well as a 500bp promoter fragment were generated in the same manner. This resulted in the firefly *luciferase (luc)* gene in the vector backbone being driven by the inserted SB3 promoter such that a luminescence assay could be used to detect the activity of the promoter.

Transient transfections using Lipofectamine2000 were optimized for Huh7 cells, a human hepatoma cell line. Cells expressing GFP in an unoptimized transfection (left) and an optimized one (right) at 48hrs post transfection, the time point at which maximal expression was found is shown in Figure 2.2A. In order to optimize the transfection efficiency to approximately 40%, all aspects of the protocol were modified. First, it was determined that the DNA Maxiprep elution buffer and the Lipofectamine2000 showed buffer incompatibility, so all the promoter constructs were precipitated out and redissolved in MilliQ H_2O. This resulted in increased expression of the transfected gene since a greater percentage of DNA was being incorporated into the liposomes and subsequently being taken up by the cells. Secondly, the seeding density of the Huh7 cells was increased in the 12 well culture dish from $5.5*10^4$ cells/mL to $7.5*10^4$ cells/mL. Also, cells were incubated for a full 24hrs before starting the transfection. This ensured confluence of 95% before beginning the transfection and greatly improved cell viability at 48hrs post transfection. Thirdly, the concentration of plasmid DNA and Lipofectamine2000 were decreased from the manufacturer's recommended protocol for a 12 well dish (1.6µg DNA with 4µL of Lipofectamine2000 per 200µL OPTI-MEM) to the recommended protocol for a 24 well dish (0.8µg DNA with 2µL of Lipofectamine2000 per 100µL OPTI-MEM) while maintaining 1mL of media on the cells. This reduced the cytotoxicity of the Lipofectamine2000 and increased overall cell viability. And lastly, the transfection was performed by diluting the DNA and Lipofectamine2000 in OPTI-MEM 1x reduced serum

media and adding it to the overnight growth media as opposed to removing the overnight media and plating cells with OPTI-MEM and the transfection mixture. This meant that antibiotics had to be excluded from the overnight growth media for optimal transfection efficiency, but were added back into the media for the 48hr incubation period post transfection. These combined modifications resulted in not only a greater expression of the transfected DNA, as seen by the GFP fluorescence but also greater cell viability, as seen by the number and morphology of the Huh7 cells (Figure 2.2A).

Once the transient transfection was optimized, the SB3-pGL3 basic plasmids (5Kb to 0.5Kb) were transfected into Huh7 cells, along with the pRL-TK *renilla* luminescence plasmid used as an internal transfection control. Figure 2.2B shows the activity of the SB3 promoters which were standardized to *renilla* and reported as a percentage of the SB3 5Kb promoter, which was arbitrarily standardized to 100%. Activity of the truncated promoter fragments decreased as compared to the SB3 5Kb promoter which showed weak activity in Huh7 cells as compared to the robust Hepc 2.7Kb-pGL3 promoter. Cells transiently transfected with the SB3 5Kb promoter were treated overnight with 5ng/mL human recombinant IL-6 (Figure 2.2C). Despite a significant 2-fold induction of Hepc 2.7Kb-pGL3 ($p<0.001$), no induction of the SB3 promoter was seen.

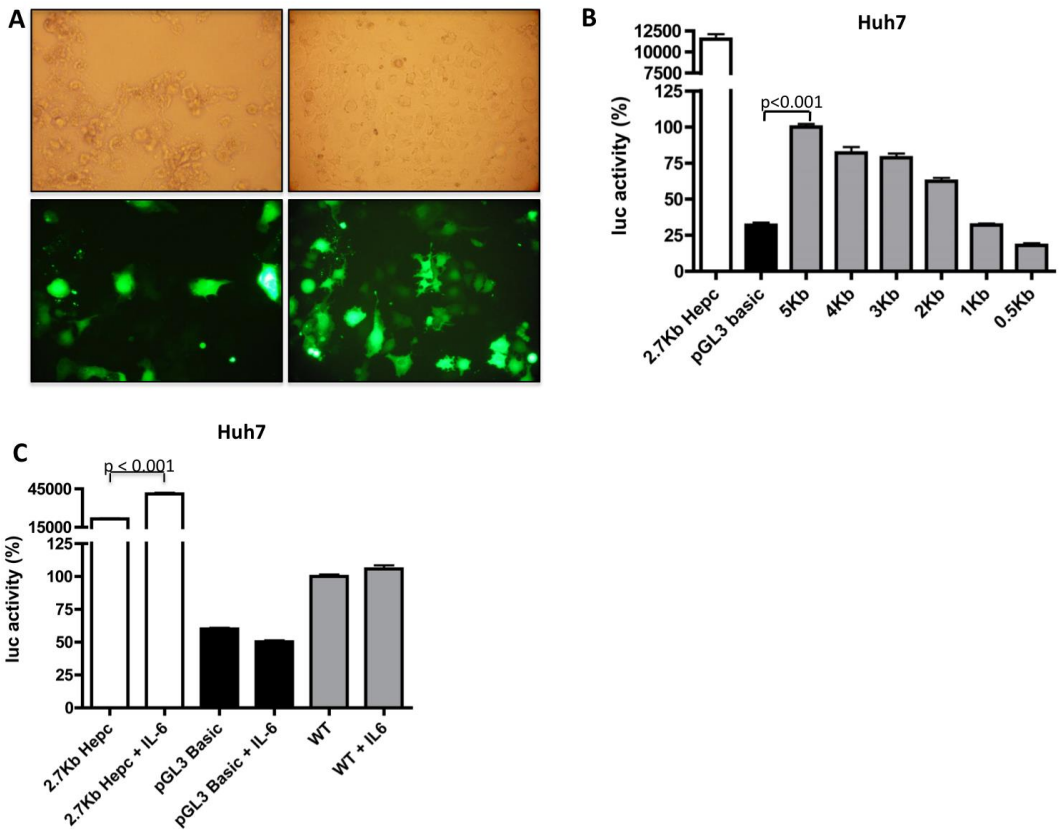

Figure 2.2: SERPIN B3 promoter activity is weak in Huh7 cells.

(A) Transient transfections of Huh7 cells using Lipofectamine2000 were optimized using a GFP expression plasmid. Transfection efficiency was increased from 20% (left) to approximately 40% (right) and was coupled with nearly a 4-fold increase in cell viability, as seen by the cell morphology (top). (B) Transient transfections of SB3 promoter fragments into Huh7 cells show it to be a weak promoter as compared to the robust Hepc 2.7Kb-pGL3 promoter. A decrease in SB3 promoter length was coupled with a decrease in *luciferase (luc)* luminescence. (C) Interleukin-6 (IL-6) treatments on the SB3 5Kb promoter transiently transfected into Huh7 cells shows no induction of *luc* despite a significant 2-fold Hepc 2.7Kb-pGL3 activation with the treatment ($p<0.001$).

2.5.2 SERPIN B3 promoter is unresponsive to iron and oxidative stress *in vitro*

To determine iron dependent regulation on the promoter of SB3, Huh7 and HeLa cells transfected with the SB3 5Kb promoter construct were treated with two different iron sources and an iron chelator. Overnight treatment with 50µM hemin (a heme-like iron source), 3µg/mL ferric ammonium citrate (FAC) (a 'free' iron source), or 100µM deferoxamine (DFO) (an iron chelator) showed a significant but mild 1.5-fold induction of SB3 promoter activity with the hemin treatment in both Huh7 and HeLa cells ($p<0.001$ and $p<0.05$ respectively) (Figure 2.3A). Neither FAC nor DFO treatments resulted in induction or suppression the of SB3 promoter. The Hepc 2.7Kb-pGL3 promoter used as a positive control shows a 15-fold decrease in activity when transfected into HeLa cells as compared to Huh7 cells; this is consistent with the fact that Hepc is predominantly expressed in hepatocytes.

To verify that the iron treatments were adequately delivering iron to the cells, western blots were performed on untransfected cells treated overnight with the iron sources and chelator. As expected, ferritin, the intracellular iron storage protein, was increased in both hemin and FAC treated cells but not in DFO treated cells (Figure 2.3B top). Also as expected, heme oxygenase 1 (HO-1), the enzyme catalyzing the degradation of heme and the removal of its ferrous iron, was induced with hemin treatments and was coupled with an increase in ferritin (Figure 2.3B bottom).

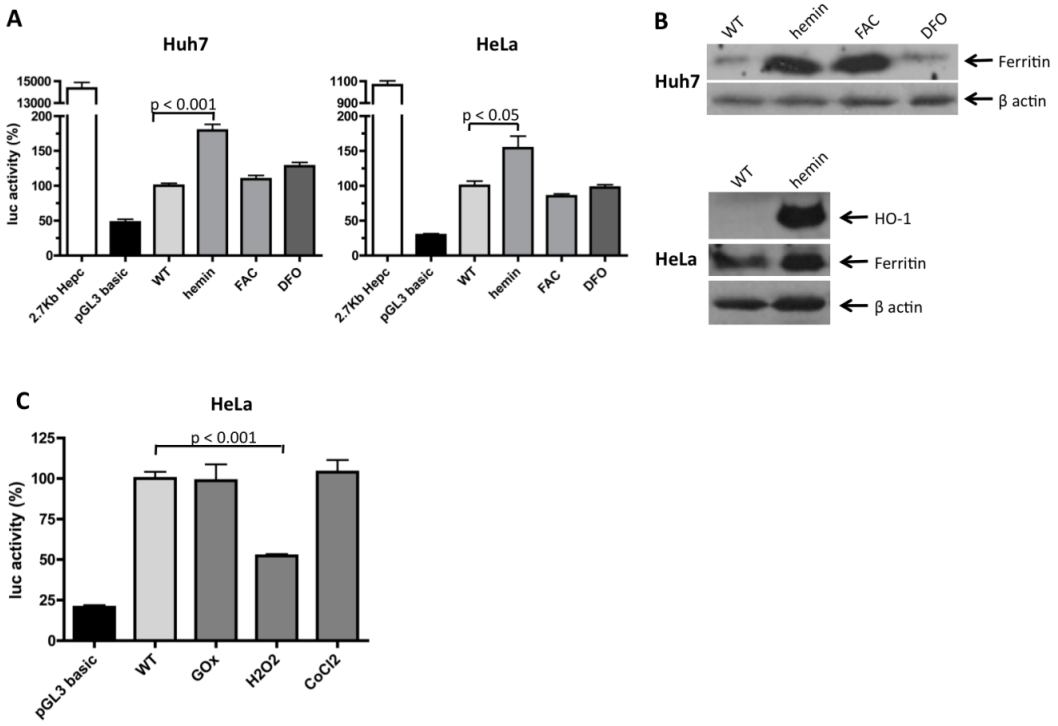

Figure 2.3: SERPIN B3 promoter treated with iron sources or chelator and oxidative stress agents shows only mild induction with hemin. (A) The SB3 5Kb promoter was transiently transfected into either Huh7 or HeLa cells and cells were then treated overnight with the iron sources hemin (50µM) or ferric ammonium citrate (FAC) (3µg/mL), or with the iron chelator deferoxamine (DFO) (100µM). A mild but significant induction of SB3 promoter activity was seen with hemin treatments in both Huh7 and HeLa cells ($p<0.001$ and $p<0.05$ respectively) but no induction or suppression was observed with either FAC or DFO. (B) Western blots for ferritin (Ft) with β-actin control showed an increase in Ft for both iron treatments but not with iron chelation treatment (top). Hemin treatment also induced heme oxygenase 1 (HO-1) expression, which is coupled to an increase in Ft (bottom). (C) HeLa cells transfected with the SB3 5Kb promoter and treated with oxidative stress (OS) inducer molecules hydrogen peroxide (H_2O_2) (500µM), cobalt (II) chloride ($CoCl_2$) (100µM), or glucose oxidase (GOx) (0.025U/µL) for 6hrs showed no induction of *luciferase (luc)* but a mild but significant suppression with H_2O_2 ($p<0.001$).

Since *in vitro* induction of the SB3 promoter with the iron treatments was not seen, HeLa cells were treated with oxidative stress agents. It was hypothesized that iron could be exerting its effect on SB3 seen *in vivo* via an intermediate, and iron has a known capacity to catalyze the generation of ROS. HeLa cells were used specifically here for two reasons. Firstly, they are a cell line originally derived from cervical epidermoid carcinoma, which is also known as squamous cell carcinoma (SCC), and therefore were shown to express endogenous SB3 mRNA whereas Huh7 cells show no endogenous SB3 mRNA expression (Figure 2.4). Secondly, endogenous SB3 mRNA expression was increased with hemin treatments (Figure 2.4) and hemin is known to catalyze the generation of ROS as does 'unshielded' iron. HeLa cells were treated with either 20µM menadione (a free radical generator), 0.025U/µL glucose oxidase (GOx) (the enzyme that catalyzes the breakdown of glucose with the production of hydrogen peroxide as a by-product), 500µM hydrogen peroxide (H_2O_2), or 100µM cobalt (II) chloride ($CoCl_2$) (an activator of hypoxia inducible factors (HIFs)) for 6hrs two days post transient transfection with the SB3 5Kb promoter (Figure 2.3C). Cells were checked visibly for signs of treatment effectiveness (a decrease in fibroblastic projections such that cells appeared sphere-like on the culture dish), as well as with H_2O_2 indicator strips for GOx and H_2O_2. The single dose of H_2O_2 was cleared from the cells in under 30mins from the starting concentration of approximately 17 mg/L H_2O_2 to less than 0.5 mg/L as measured from the peroxide strips. The GOx produced a continuous supply of H_2O_2, which was below 0.5mg/L for the first hour of treatment, but then plateaued at approximately 2mg/L. For all four treatments, cell morphology looked normal for the first 2-3hrs of treatment, but then a drastic decrease in fibroblastic projections was observed for the last 3hrs of the treatment. The 20µM menadione treatment, while effectively generating OS, was too toxic for the cells and the luciferase assay was below the detection limits of the luminometer. The GOx and $CoCl_2$ treatments showed no induction of the SB3 promoter whereas H_2O_2 treatment slightly but significantly suppressed SB3 promoter activity by 2-fold ($p<0.001$).

2.5.3 Endogenous SERPIN B3 is weakly expressed in cell lines and is non-responsive to iron *in vitro*

To determine if SB3 transcription was responsive to iron *in vitro*, real time PCR (qPCR) was performed on Huh7, HeLa, and HA22T/VGH, a liver endothelial cell line, cells. Cells were treated overnight with either 50µM hemin, 3µg/mL FAC, or 100µM DFO (Figure 2.4). Huh7 cells did not express endogenous SB3 mRNA, whereas HeLa and HA22T/VGH cells showed low expression as compared to the GAPDH control gene. Treatment of the HA22T/VGH cells with iron showed no significant induction of the SB3 gene with iron treatments or suppression with the iron chelator, whereas HeLa cells showed a significant 6-fold induction of SB3 mRNA with hemin treatments ($p<0.001$) but no change with either FAC or DFO treatments.

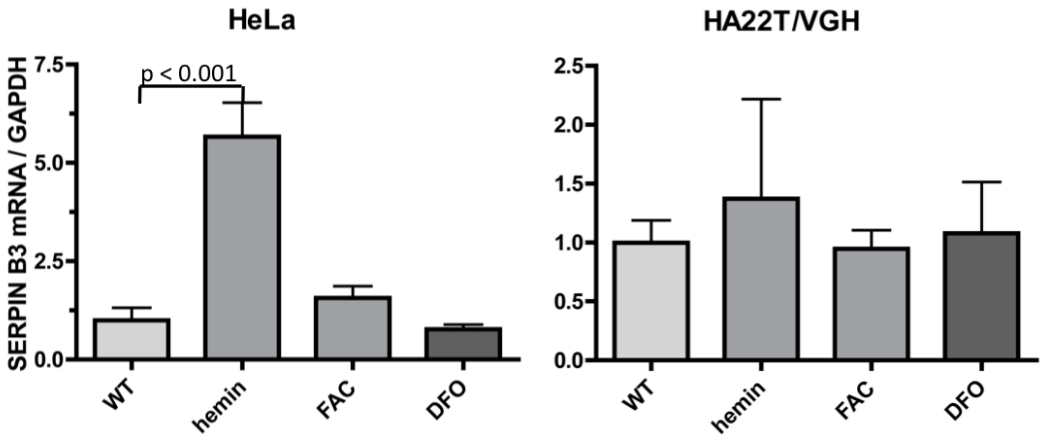

Figure 2.4: SERPIN B3 is weakly expressed in cell lines. qPCR was performed on HeLa, HA22T/VGH, and Huh7 cells for SB3 mRNA expression as compared to GAPDH control gene and reported as fold changes from untreated (WT) cells. HeLa and HA22T/VGH cells showed low expression of SB3 mRNA whereas Huh7 cells do not express it. HA22T/VGH cells treated overnight with hemin (50µM), FAC (3µg/mL), or DFO (100µM), showed no induction or suppression of the SB3 gene with any treatment. The same treatments on HeLa cells showed a 6-fold induction of SB3 with only the hemin treatment ($p<0.001$).

2.5.4 Does SERPIN B3 function as an upstream regulator of hepcidin?

To determine if SB3 acts upstream of hepcidin (Hepc), stable clones of HJV in Huh7 cells were generated. First, HJV WT-pUHD10.3 and G320V-pUHD10.3 plasmids, expressing the HJV WT and G320V mutant cDNA under control of the tet-inducible promoter (TRE fused to P_{min}CMV) in the pUHD10.3 vector were transiently transfected into Huh7-tTA cells. The G320V mutant of HJV was used since it is the most common mutation seen in patients with Type II HH. This amino acid substitution is at a highly conserved residue and affects the protein folding and therefore its functionality. The Huh7-tTA cells used already stabily express the tTA protein, which in the absence of 2µg/mL of tetracycline (tet) binds to the TRE element of the promoter and drives gene expression. Cells were grown for 72hrs with the addition or elimination of tet in the media. Figure 2.5A shows tight control with the addition of tet completely abolishing gene expression with both the HJV WT and G320Vmutant.

Next, the HJV WT-pUHD10.3 and G320V-pUHD10.3 plasmids were co-transfected with the pBABE-puro plasmid at a ratio of 10:1 using Lipofectamine2000. Three days post transfection, Huh7-tTA cells were split at sequential dilutions and grown for approximately one month in regular media with 250µg/mL G418 (to maintain the tTA gene), 2µg/mL puromycin (to select for positive clones), and 2µg/mL tet (to turn off HJV gene expression). Single cells that had resistance to both antibiotics formed colonies that were picked up and expanded. These clones were grown with or without tet for 72hrs and HJV protein expression was determined via Western blot. Figure 2.5B shows a representative blot of both WT and G320V mutant HJV stable clones. Of the approximately 70 clones expanded no clone showed sufficiently high levels of HJV protein expression, especially when compared to the H1299-HJV cells generated previously in the laboratory and used as a positive control.

Since the double plasmid method of generating stable clones was unsuccessful, the HJV WT and G320V mutant cDNA was cloned into a vector expression both

the TRE promoter and antibiotic resistance gene (hygromycin); the pTRE2hyg2-Myc plasmid. This vector also has an N-terminal Myc tag. After cloning and sequencing to determine the correct orientation and fusion of HJV to the Myc tag, Huh7-tTA cells were transiently transfected with the new HJV WT-pTRE2hyg2-Myc and G320V-pTRE2hyg2-Myc plasmids. Cells were treated for 72hrs with and without 2µg/mL tet in the media and protein expression was determined using Western blot for the Myc tag (Figure 2.5C). While both HJV WT and G320V mutant cDNA were expressed in the absence of tet, there was no tight control of the protein expression in the presence of tet, and therefore no attempt to generate stable clones from these plasmids was made.

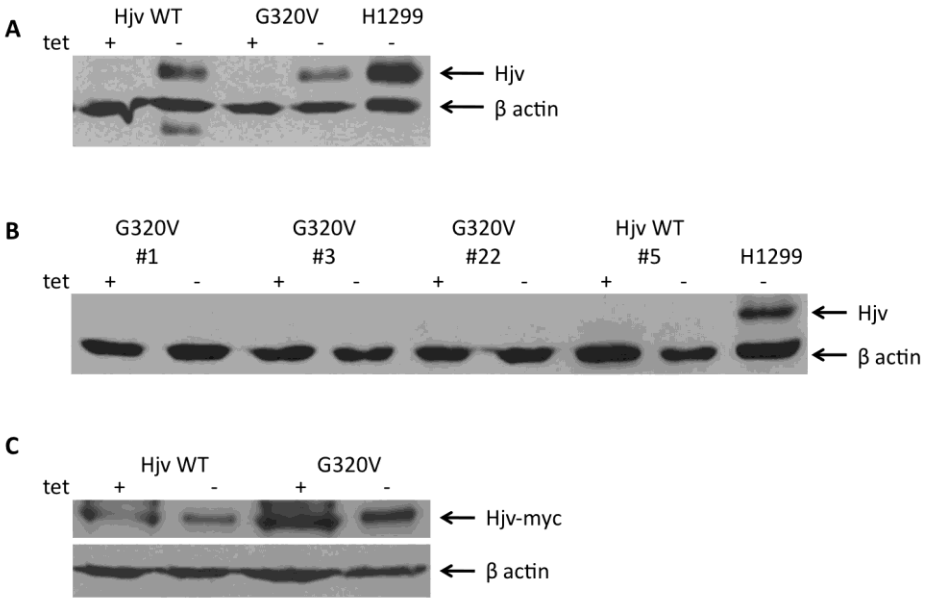

Figure 2.5: Huh7-tTA cells stabily expressing HJV WT and G320V mutant cDNA. (A) Western blot of the Huh7-tTA transient transfection of HJV WT and G320V mutant cDNA under the control of a tet-responsive promoter in the pUHD10.3 vector. Cells showed tight control of gene expression with the addition (+) or omission (-) of 2 µg/mL of tetracycline (tet). (B) Western blot for Huh7-tTA cells showed no clone expressing either HJV WT or G320V protein either with (+) or without (-) tet. (C) HJV WT and G320V mutant cDNA cloned into pTRE2hyg2-Myc plasmid and transiently transfected into Huh7-tTA cells showed no tight control of either protein expression by tet.

Instead, to determine the possible function of SB3 upstream of Hepc via cleaving TMPRSS6, triple transfections were performed. Ideally the stable clones expressing tet-inducible HJV would have been used for this experiment, but instead WT HJV-Myc, TMPRSS6-FLAG, and SB3-V5 along with each of their mutants HJV G320V-Myc, TMPRSS6 MASK-FLAG, and SB3 dHinge-V5, were transiently transfected together into Huh7 cells. Western blots for the tagged proteins were unsuccessful for a few reasons. Low transfection efficiency of Huh7 cells with Lipofectamine2000 (approximately 40% for one plasmid) resulted in too low of a concentration of cDNA being introduced into the cells and not enough protein product being generated. Also, within each cell, it could not be verified that all three plasmids were introduced in the desired 1:1:1 ratio if at all such that western blots were looking at an unhomogenous cell population.

2.6 DISCUSSION

The work performed by our collaborators in Dr. Pontisso's laboratory showed that SB3 mRNA was overexpressed in the livers of $HJV^{-/-}$ as compared to WT mice (Figure 2.1A). It was also found that in both $HJV^{-/-}$ and WT mice, SB3 mRNA expression was positively regulated with dietary iron (Figure 2.1B). Furthermore, the increase in SB3 mRNA expression correlated with an increase in protein expression, seen by immunohistochemistry of liver samples from $HJV^{-/-}$ mice on a high iron diet (Figure 2.1C). Therefore, this positive regulation of SB3 mRNA by iron *in vivo* was investigated *in vitro* at the level of transcription.

In order to determine the effects of iron on the promoter of SB3 *in vitro*, and therefore the apparent iron inducible phenotype at the level of transcription, Huh7 cells were transiently transfected with SB3-pGL3 promoter constructs. Huh7 cells were used since they are a cell line derived from the hepatocytes of a human hepatoma. Therefore, the liver specific induction of SB3 by iron in the $HJV^{-/-}$ mice could be investigated in culture, using these particular cells. However, Huh7 along with other human hepatoma cell lines are more difficult to transfect than most cell lines, with optimized liposome transfection efficiencies rarely

reaching 50%. For this reason, Lipofectamine2000 transfections had to be optimized for use in Huh7 cells, with optimal efficiency reaching 40% (Figure 2.2A).

To generate the promoter constructs of SB3, fragments immediately upstream of the transcription start site of *SB3* were cloned into the promoterless pGL3 basic *luciferase* (*luc)* reporter vector. The maximum SB3 promoter length that was cloned was 5Kb, with truncated fragments of 1Kb each and one 0.5kB fragment. When these SB3 promoter constructs were transiently transfected into Huh7 cells, they showed weak activity (Figure 2.2B). As the promoter was truncated, *luc* activity decreased, in contrast to previous findings [124, 125]. This is likely due to the group's transfection of a set amount of each promoter plasmid. So with the smaller plasmids more *luc* gene copies were being transfected. Here, transfection of equi-molar amounts of the promoter was performed which resulted in an equal amount of *luc* gene copies and a truer representation of promoter activity. The weak activity of the SB3 promoter is likely due to the fact that Huh7 cells do not express endogenous SB3 (Figure 2.4) or possibly because elements of the promoter are missing. Promoters are complex stretches of DNA that can extend far upstream of the transcription start site of the gene, but also downstream of the gene sometimes. There is the possibility that 5Kb upstream is not representative of the entire SB3 promoter or elements are present downstream of the transcription start site that would significantly increase the promoter activity [124]. This is highlighted in the treatment of Huh7 cells with IL-6 (Figure 2.2C), since no induction of *luc* was seen despite its known induction of SB3 via binding of pSTAT3 to the promoter [116]. IL-6 treatment functionality was confirmed with the 2-fold induction of the 2.7Kb Hepc-pGL3 promoter being observed [126]. However, since Huh7 cells do not express SB3, the lack of IL-6 induction could also be due to the lack of another molecule in the cell line that is required for STAT3 mediated induction of this gene. This is particularly pertinent since most groups look at SB3 in cell lines that express it, notably SKGIIIa, whereas here the particular role of SB3 in hepatocytes is under investigation.

Despite the weak activity of the SB3 promoter, it did show a mild but significant induction with hemin treatments, a heme-like iron source (Figure 2.3A). In both Huh7 and HeLa cells, the same 1.5-fold induction of the promoter was seen with hemin treatments. FAC treatments, a 'free' iron source, did not induce SB3 expression at the level of transcription, nor did DFO treatments, an iron chelator, suppress SB3 expression. This was an unexpected finding due to the previous *in vivo* data. The activity of the 2.7Kb Hepc-pGL3 promoter is 15-fold less when transfected into HeLa cells as opposed to Huh7 cells. This is likely due to the hepatocytes being the body's main producer of Hepc [53] and therefore the recognition of the promoter and vigorous transcription of the *luc* gene in the Huh7 cells. However in HeLa cells the opposite is true. This highlights the link between endogenous expression of a gene and promoter recognition and therefore subsequent gene expression.

To determine if *in vivo* iron regulation of SB3 mRNA could be shown *in vitro* beyond the level of transcription, endogenous expression of SB3 in Huh7, HeLa, and HA22T/VGH cells was investigated. It was found that Huh7 cells do not express SB3, consistently with similar data previously obtained with human HepG2 hepatoma cells [127]. HeLa, a cell line derived from cervical epidermoid carcinoma, which is also known as squamous cell carcinoma (SCC), and HA22T/VGH, a liver endothelial cell line, both express SB3 (Figure 2.4). However, only HeLa cells responded to iron treatments and like in the promoter assays, the cells only responded with hemin treatments, showing a significant 6-fold induction of SB3 mRNA.

The endogenous induction of SB3 mRNA with hemin treatments in HeLa cells coupled with the mild induction of the SB3 promoter with hemin treatments raised the possibility of a secondary effect of iron generating the robust SB3 mRNA expression *in vivo*. Notably, iron and heme can both catalyze the production of reactive oxygen species (ROS) resulting in oxidative stress (OS) and damage to the cell [8-12, 128]. It is yet not understood why hemin and FAC

treatments resulted in different induction of the SB3 promoter. To test this secondary iron effect hypothesis HeLa cells were treated with OS generating agents. HeLa cells were specifically used here since they showed the strongest induction of endogenous SB3 mRNA expression with hemin treatments (Figure 2.4). Treatment of cells with hydrogen peroxide (H_2O_2), glucose oxidase (GOx) (the enzyme that catalyzes the breakdown of glucose releasing H_2O_2 as a by-product), menadione (a free radical generator), or cobalt (II) chloride ($CoCl_2$) (an activator of hypoxia inducible factors (HIFs)) resulted in no induction of the SB3 promoter (Figure 2.3C). This implies that the hemin induced expression of SB3, both at the level of transcription on the promoter and on endogenous mRNA in HeLa cells was not due to the generation of OS but by another pathway.

Since the expression of SB3 mRNA *in vivo* was seen to be regulated by iron in $HJV^{-/-}$ mice, the possibility of SB3 functioning upstream of Hepc was investigated. Stable clones expressing HJV and G320V mutant cDNA were attempted, however no clone was found to express HJV at a suitable level (Figure 2.5B) despite tight control of protein expression with tet with transient transfections of the plasmids (Figure 2.5A). Therefore, triple transient transfections of the SB3, TMPRSS6, and HJV cDNA were attempted. Due to low transfection efficiency in Huh7 cells (40% at maximum, Figure 2.2A) detection of the proteins was not successful since too low of a concentration of cDNA was introduced into the cells. Therefore the experiment to determine if SB3 functions upstream of Hepc by cleaving TMPRSS6 neither proved nor disproved the hypothesis. Since SB3 specifically inhibits papain-like cysteine proteases [111], it appears unlikely that it would inhibit the serine protease TMPRSS6. Nevertheless, this remains to be validated experimentally.

In conclusion, the lack of iron-dependent induction of the SB3 promoter and the weak induction of *SB3* gene expression indicates that the robust iron-dependent regulation of SB3 mRNA seen in the $HJV^{-/-}$ mice liver is not caused by cell autonomous transcriptional regulation.

CHAPTER 3

A novel HFE and HJV double knockout mouse demonstrates crosstalk between the proteins for induction of hepcidin

3.1 PREFACE

Rational of the study:

Upstream regulatory elements of hepcidin are numerous and complex, including two iron sensing pathways. While much has been learned in the last ten years there are still some questions to be addressed with regards to the mechanisms of hepcidin induction. Several mouse models have been generated bearing targeted disruption of key iron genes, including those which cause hereditary hemochromatosis in humans when inactivated. However, not enough is currently understood about the intracellular signalling cascades and the potential interaction between the iron sensing pathways that fine tune hepcidin expression.

3.2 ABSTRACT

Hereditary hemochromatosis is the result of genetic mutations in key proteins in the iron regulatory pathways. It is characterized by elevated levels of serum iron, hepatic iron deposition, an increase in dietary iron uptake, and blunted levels of hepcidin expression. Left untreated it can result in tissue damage, especially to the liver, due to the overabundance of unshielded iron in the body. Hepcidin is the liver derived peptide hormone which plays a central role in modulating systemic iron movement by blocking iron efflux from cells. Since hepcidin orchestrates this systemic iron homeostasis, it must be tightly controlled to maintain the balance of iron between storage, recycling, and utilization. In part, hepcidin is modulated by iron via two pathways in hepatocytes; serum iron and hepatic iron. *In* vitro data indicates that serum iron is sensed via proteins on the plasma membrane, one of which is the human hemochromatosis protein (HFE). Hepatic iron sensing also starts at the membrane, with hemojuvelin (HJV) playing a key role. Then an intracellular signalling cascade involving the BMP/SMAD proteins induces hepcidin expression to lower serum iron concentration and decrease dietary iron uptake. Here, we investigated the effects of knocking out both *HFE* and *HJV* genes in mice. This novel double knockout (DKO) had serum iron parameters like the single $HJV^{-/-}$, which were elevated compared to both $HFE^{-/-}$ and wildtype (WT). When these mice were challenged with a high iron diet, serum iron parameters were further elevated, but no differences between DKO and $HJV^{-/-}$ mice were observed. Hepatic iron loading indicated that both $HJV^{-/-}$ and DKO mice accumulated the same amount of iron, which was significantly more than either WT or $HFE^{-/-}$. Hepcidin expression was also severely attenuated in these mice, and inappropriately low compared to the immense hepatic iron loading. Further, other downstream targets of the BMP/SMAD pathway were particularly decreased in the DKO, as compared to the $HFE^{-/-}$ and $HJV^{-/-}$ mice. Taken together, this set of data shows that there is definitive crosstalk between the HFE- and Hjv-mediated signalling cascades, which most likely appears early in the BMP/SMAD pathway.

3.3 INTRODUCTION

Iron is an essential element for life, yet it can also be toxic in biological systems. If iron is left unshielded it can catalyze the formation of reactive oxygen species (ROS) via Fenton and Haber-Weiss reactions [8, 9]. Then the ROS will generate oxidative stress (OS) to damage DNA, proteins, and lipids within the cell [10-12]. What further complicates the necessity yet toxicity of iron is the fact that there is no regulated iron excretion system in mammals [14]. Iron is only lost via the sloughing of epithelial cells from the skin and intestinal tract and though blood loss [15]. Therefore the uptake of iron from the diet must be controlled to only compensate for daily loses of the metal [17]. This results in a tightly controlled recycling system of iron within the body as well as a system to safely move iron between the cells that utilize, recycle, and store the metal [129].

Hepcidin (Hepc) was originally discovered as an anti-microbial peptide [51], but it is now known to be the liver-derived peptide hormone that is the master regulator of systemic iron homeostasis. The Hepc that is in circulation is primarily produced by hepatocytes. The 84 amino acid pre-prohepcidin precursor undergoes cleavage by furin to yield the biologically active 25 amino acid peptide [52]. Hepc orchestrates the tight control of iron movement throughout the body by controlling iron efflux from cells [56]. It does this by binding to ferroportin (FPN) which is the only known iron exporter [30-32]. Once the binding occurs, the Hepc-FPN complex is internalized where it undergoes ubiquitin dependent lysosomal degradation [56]. Since FPN is expressed on the enterocytes of the intestinal duodenum (the cells responsible for dietary iron uptake) [33], macrophages (the cells that phagocytize senescent red blood cells and release iron from heme) [130], and hepatocytes (the cell that store most of the body's iron in ferritin (Ft)) [131], Hepc can control all aspects of iron movement by targeting FPN.

Since Hepc plays such a pivotal role in iron homeostasis, its expression too must be tightly controlled to maintain the balance of iron. Hepc is controlled via four

known sources; hypoxia, inflammation, erythropoiesis, and iron. Inflammatory cues are thought to be a mechanism of host defence against invading pathogens, who have a rapidly dividing population and therefore have a high iron demand such that they can grow and multiply [132]. Erythropoiesis cues are thought to be secreted from maturing erythroid precursors [50] ensuring that there is enough iron to incorporate into heme and produce functional red blood cells. Iron cues to Hepc expression are quite complex and are a result of sensing both circulating serum iron and hepatic iron stores [133].

An attractive model postulates that serum iron is sensed via three proteins on the cell membrane of hepatocytes; the hereditary hemochromatosis protein (HFE), transferrin receptor 1 (TfR1), and transferrin receptor 2 (TfR2) [58, 59]. Serum iron is not 'free', but bound to transferrin (Tf) [36] to keep it redox inactive as well as soluble at physiological pH 7.4 [13]. Two ferric (Fe^{3+}) iron atoms bind to each Tf [37] and this holo-transferrin complex can signal to Hepc. A signalling cascade only occurs when serum iron concentrations are elevated, indicating that iron should not be absorbed from the diet via enterocytes, released from macrophage recycling, or released from storage in the hepatocytes. The cascade begins with holo-transferrin displacing HFE from its association with TfR1 since both share overlapping binding sites on TfR1 [60, 61]. This frees HFE to associate with TfR2, which also binds holo-transferrin [62, 63]. Then a poorly understood intracellular signalling cascade possibly involving the bone morphogenetic protein (BMP)/ Homologs of both the *Drosophila* protein Mothers Against Decapentaplegic and the *C. elegans* protein SMA (SMAD) and/or mitogen-activated protein kinases (MAPK) pathways ensues [64-66]. The end result of the signalling cascade is an increase in Hepc expression and therefore a decrease in serum iron levels.

Hepatic iron sensing and signalling to Hepc also involves membrane bound proteins and an intracellular signalling cascade. It starts with BMP6 mRNA expression being positively regulated by liver iron content and the protein is

secreted into the plasma where it can bind its BMP receptor [67, 68]. Hemojuvelin (HJV) acts as a co-receptor for BMP6, enhancing the downstream signalling cascade [69]. SMAD 1/5/8 becomes phosphorylated and forms a complex with SMAD4 which translocates to the nucleus [73]. The complex then binds to proximal and distal sites on the *HAMP* (Hepc gene) promoter to induce Hepc expression [70]. As with the serum iron signalling to Hepc, the hepatic iron sensing pathway results in a decrease in serum iron and an increase in cellular iron concentrations. This is due to the increase in Hepc in circulation which binds to and causes degradation of FPN, abolishing iron efflux from enterocytes, macrophages, and hepatocytes.

In order to better understand the regulation of Hepc, a number of mouse models have been employed. $HFE^{-/-}$ mice are phenotypically like hereditary hemochromatosis (HH) type I patients in that they have iron loading of the liver, increased transferrin saturation levels, and decreased expression of Hepc especially when considering body iron load [134, 135]. HH type III is rare and the result of mutations in *TfR2* which presents with a more severe phenotype than type I [85]. $TfR2^{-/-}$ mice accordingly show a more severe phenotype than $HFE^{-/-}$ mice in that they have increased hepatic iron loading, further suppression of Hepc expression, an increase in transferrin saturation, and an increase in dietary iron absorption [136-138]. Interestingly, the double $HFE^{-/-}/TfR2^{-/-}$ mouse has a phenotype that most closely resembles HH type II, also known as juvenile HH because of its early onset and severity. The mouse shows more severe hepatic iron loading and a further decrease in Hepc expression [86]. This double knockout mouse highlights the cooperative behaviour of HFE and TfR2 since when both genes are deleted, the phenotype is the additive effects of the single knockout [86]. $HJV^{-/-}$ mice are phenotypically similar to HH type IIA patients (juvenile HH) [83]. They show the most severe hepatic iron loading as well as cardiac and pancreatic iron loading, oversaturation of serum transferrin, and profound suppression of Hepc expression, just like the combined $HFE^{-/-}/TfR2^{-/-}$ mouse [75]. What is important to note in the use of mouse models to study HH

resulting from altered Hepc expression is that there are natural strain to strain variations. The mouse background is particularly important in iron loading and therefore basal serum transferrin saturation levels and Hepc expression [139, 140].

While a number of knockout mouse models have been generated to look at the known key proteins in iron sensing to hepatic Hepc, no mouse model has yet addressed the possibility of HFE and HJV acting cooperatively. It is known that pSMAD 1/5/8 and pSMAD4 play a key role in the BMP6/HJV mediated signalling to Hepc. They are thought to play a role in HFE mediated signalling as well and thus could be link between the two pathways [66]. To address this question of crosstalk in Hepc induction mediated by HFE- and HJV-dependent signalling, we generated a novel knockout mouse with deletions in both *HFE* and *HJV* and looked at serum iron parameters, tissue iron loading, and Hepc expression. Of specific interest is how this double knockout (DKO) mouse of *HFE* and *HJV* would compare to the single knockouts and if it would demonstrate cooperativity of the two proteins in Hepc signalling.

3.4 MATERIALS AND METHODS

3.4.1 Animals

C57BL/6 mice were purchased from Jackson Laboratories. $HJV^{-/-}$ mice were a kind gift from Dr. N. Andrews [75] and backcrossed onto the C57BL/6 background in our laboratory [141]. $HFE^{-/-}$ mice were a kind gift from Dr. M. Santos, who backcrossed them onto the C57BL/6 background, but were originally generated by Dr. N. Andrews [142]. The double knockout (DKO) mice were generated by crossing the $HFE^{-/-}$ and $HJV^{-/-}$ mice. Mice were housed in macrolone cages (up to 5 mice per cage, 12:12-hr light-dark cycle, 22±1°C, 60±5% humidity) according to institutional guidelines. Mice were given free access to water and a standard rodent diet, containing approximately 225mg of

iron per kg (Harlan Laboratories). For iron challenge studies, 6 week old mice were maintained on a standard diet containing 2% carbonyl iron (5.6g iron per kg) (Harlan Laboratories) for 4 weeks. Male mice (n=8) were used in experiments and were sacrificed at 10 weeks of age by CO_2 inhalation. This is due to the fact that there are gender based differences in iron loading [143] and iron levels plateau at 10 weeks of age [144]. Experimental procedures were approved by the Animal Care Committee of McGill University (protocol 4966).

3.4.2 CBC Measurements

Whole blood (25µL) was collected via cardiac puncture and stored in a microvette (Sarstedt) until analysis. Complete blood count (CBC) values were acquired with the Scil Vet-ABC hematology analyzer.

3.4.3 Serum Biochemistry

Blood was collected via cardiac puncture and clotted at room temperature for 1hr. Serum was obtained via centrifugation at 2000xg for 10 mins before being snap frozen in liquid nitrogen and stored at -80°C. The biochemistry department of the Jewish General Hospital measured serum iron, serum ferritin, and total iron binding capacity (TIBC) using a Roche Hitachi 917 Chemistry Analyzer. Transferrin saturation was calculated from the ratio of serum iron and TIBC.

3.4.4 Ferrozine Assay

Livers were collected, snap frozen in liquid nitrogen, and stored at -80°C until quantification of non-heme iron was performed with the ferrozine assay. Frozen tissue was cut and dried overnight at 106 ºC. Dry tissue was massed (g dry tissue) and approximately 10mg was diluted in 500µL acid mixture (3M HCl, 10% TCA) and incubated at 65ºC for 48hrs. Supernatant was collected via centrifugation at 10,000xg for 5 mins. In a 96 well plate, 50µL of supernatant was diluted in 200µL ferrozine reagent (4mM ferrozine reagent, 89mM ascorbate, 1.05M sodium acetate) and incubated at room temperature for 30mins. Absorbance at 562nm was measured and compared to a standard curve obtained from $FeCl_3$

(QuantiChrom Iron Assay Kit, BioAssay Systems). Tissue iron values are expressed as µg iron per g of dry tissue weight.

3.4.5 Atomic Absorption Spectrometry

Liver and spleen were collected, snap frozen in liquid nitrogen, and stored at -80°C until quantification of total iron, both non-heme and heme bound, was performed with atomic absorption spectrometry. Crucibles were dried overnight at 160 ºC in an oven and weighed (g empty crucible). Samples were placed in crucibles, and weighed again (tissue wet weight) before overnight drying at 106 ºC in an oven. Crucibles were placed in a desiccator for 1hr until samples had reached room temperature, and weighed again (g dry weight). Samples were ashed overnight at 500ºC in a furnace before extraction in 1mL 6N HCl and appropriate dilution in double distilled water (ddH_2O) and vortexed thoroughly. Iron content was measured with an AAnalyst 200 flame atomic absorption machine (Perkin Elmer) by the Geology Department of the Université de Montréal.

3.4.6 qPCR

Total RNA was extracted with TRIzol (Invitrogen) as per the manufacturer's protocol from liver tissue snap frozen in liquid nitrogen and stored at -80°C. cDNA was synthesized from 1µg of RNA with the QuantiTect Reverse Transcription kit (Qiagen) as per the manufacturer's protocol. SYBR Green (Qiagen) and gene specific primers as in Table 3.1 were used to amplify products with the following cycling conditions: initial denaturation 95°C 10mins, 40 cycles of 95°C 30sec, 58°C 1min, 72°C 1min, and final cycle melt analysis from 58°C to 95°C for qPCR analysis. Data was normalized to β-actin reference gene and reported as fold changes.

mHAMP1 – F	AAGCAGGGCAGACATTGCGAT
mHAMP1 – R	CAGGATGTGGCTCTAGGCTATGT
mBMP6 – F	ACTCGGGATGGACTCCACGTCA
mBMP6 – R	CACCATGAAGGGCTGCTTGTCG
mId1 – F	GGTACTTGGTCTGTCGGAGC
mId1 – R	GCAGGTCCCTGATGTAGTCG
mSMAD7 – F	TCGGACAGCTCAATTCGGAC
mSMAD7 - R	GGTAACTGCTGCGGTTGTAA
mβ-actin – F	GACGACATGGAGAAGATCTG
mβ-actin – R	GTGAAGCTGTAGCCACGCTC

Table 3.1: qPCR gene specific primer sequences.

3.4.7 Statistical Analysis

Data is expressed as mean ± standard error mean (SEM). Analysis of multiple groups was performed with 1-way ANOVA and analysis of two groups was performed with the Student's t test in the Prism GraphPad software (version 5.0d). A probability value of $p < 0.05$ was considered to be statistically significant.

3.5 RESULTS

3.5.1 DKO mice resemble HJV$^{-/-}$ in serum and blood parameters

Serum iron and ferritin levels and total iron binding capacity (TIBC) were determined for 10-week old male DKO, HFE$^{-/-}$, and HJV$^{-/-}$ mice and compared to WT mice fed a standard iron diet of 225mg iron per kg (Figure 3.1A). Serum iron levels were significantly 1.4-fold higher in HFE$^{-/-}$ (50µmol/L) ($p<0.01$) and significantly 1.6-fold higher in both HJV$^{-/-}$ and DKO (both 55µmol/L) ($p<0.001$) compared to WT mice (35µmol/L). However there was no difference between the HFE$^{-/-}$ and HJV$^{-/-}$ and DKO mice (Figure 3.1A left). Serum ferritin levels in WT and HFE$^{-/-}$ mice were similar at 280µg/L and 320µg/L respectively. Levels were

significantly 2-fold higher in $HJV^{-/-}$ (520 µg/L) ($p<0.01$) and in DKO (620µg/L) ($p<0.001$) compared to WT mice (Figure 3.1A middle). Transferrin saturation was calculated from the ratio of serum iron and TIBC. Saturation levels for WT mice were 50% and were significantly lower that either $HFE^{-/-}$ or $HJV^{-/-}$ at 74% ($p<0.01$) and DKO at 89% ($p<0.001$) (Figure 3.1A right).

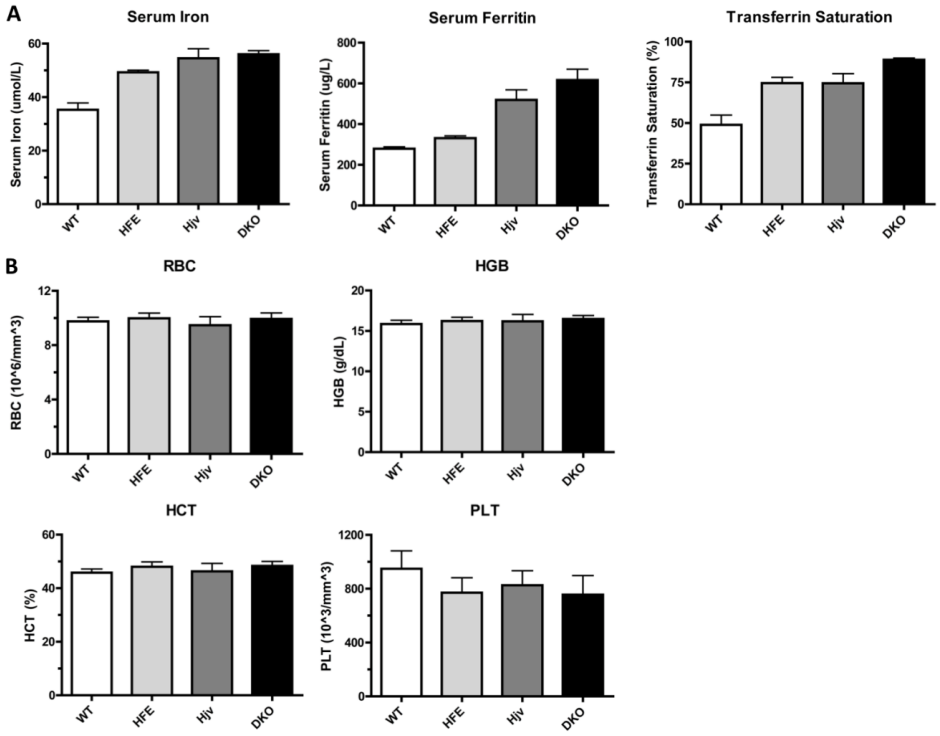

Figure 3.1: Serum and complete blood analysis of mice fed a standard iron diet. (A) Serum iron, serum ferritin, and transferrin saturation were determined for 10 week old male mice (n=8) on a standard iron diet (225mg per kg). Serum iron was significantly higher in $HFE^{-/-}$ ($p<0.01$) and in both $HJV^{-/-}$ and DKO ($p<0.001$) compared to WT mice. Serum ferritin was similar for WT and $HFE^{-/-}$ and significantly higher in $HJV^{-/-}$ ($p<0.01$) and in DKO ($p<0.001$) compared to WT. Transferrin saturation was significantly higher in $HFE^{-/-}$ and $HJV^{-/-}$ ($p<0.01$) and in DKO ($p<0.001$) compared to WT mice. (B) Complete blood count (CBC) was performed on whole blood samples from the same mice. There was no difference in RBC (red blood cell), HGB (hemoglobin), or HCT (hematocrit) between the genotypes. PLT (platelet) was slightly but not significantly lower in $HFE^{-/-}$, $HJV^{-/-}$, and DKO compared to WT mice.

Complete blood count (CBC) was performed looking specifically at the red blood cell count (RBC), hemoglobin (HGB), hematocrit (HCT), and platelet count (PLT) (Figure 3.1B). RBC was constant at $10x10^6/mm^3$, HGB was constant at 16g/dL, and HCT was constant at 45% for all genotypes. PLT was slightly lower in $HFE^{-/-}$ and $HJV^{-/-}$ ($775\ x10^3/mm^3$ and $825\ x10^3/mm^3$ respectively) and further lower in DKO ($750\ x10^3/mm^3$) compared to WT ($950\ x10^3/mm^3$), but the decrease was not significant.

3.5.2 Severe liver iron loading is seen in both $HJV^{-/-}$ and DKO mice fed a standard diet

The ferrozine assay was used to determine non-heme bound iron in the livers of WT, $HFE^{-/-}$, $HJV^{-/-}$, and DKO mice fed the standard iron diet for 10 weeks (Figure 3.2). There was a significant 5.9-fold higher level of liver iron content in $HFE^{-/-}$ (1500µg Fe/g dry liver) ($p<0.01$) as well as a significant 26-fold higher level in both $HJV^{-/-}$ and DKO (5750µg Fe/g dry liver and 5825µg Fe/g dry liver) ($p<0.001$) compared to WT mice (225µg Fe/g dry liver). However, there was no difference in liver iron content between $HJV^{-/-}$ and DKO mice.

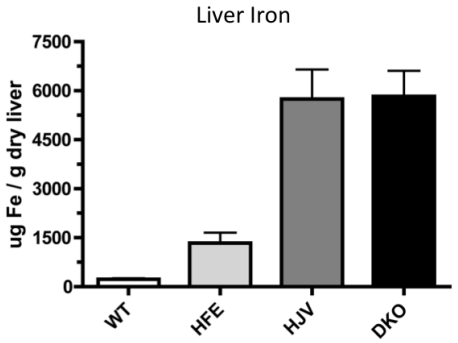

Figure 3.2: Liver iron content of mice on a standard iron diet. A ferrozine assay for non-heme bound iron was performed on liver samples from 10 week old male mice (n=8) fed a standard iron diet. There was a significantly higher levels in $HFE^{-/-}$ ($p<0.01$) and further higher levels $HJV^{-/-}$ and DKO ($p<0.001$) compared to WT mice.

3.5.3 Serum parameters of the DKO mice continue to phenocopy HJV$^{-/-}$ mice when challenged with a high iron diet

Male mice were divided into two groups at 6 weeks of age. One group continued to receive a standard iron diet of 225mg iron per kg (normal iron diet – NI) while the other was given an iron enriched diet of 5.6g iron per kg (2% carbonyl iron diet – CI). All mice (n=8) were sacrificed at 10 weeks of age and serum parameters were analysed (Figure 3.3). Serum iron was significantly higher in both WT and HFE$^{-/-}$ mice on the CI diet, 55µmol/L and 60µmol/L respectively, compared to the matched genotype mice on the NI diet, 35µmol/L and 48µmol/L ($p<0.001$ and $p<0.05$ respectively). This represented a 1.9-fold higher level for WT and a 1.25-fold higher level for HFE$^{-/-}$ between the CI and NI diets. Interestingly in HJV$^{-/-}$ mice, serum iron was 1.2-fold lower in mice on the NI diet (63µmol/L) compared to the CI diet (51µmol/L) ($p<0.05$). However, there was a non-significant change in the serum iron for DKO mice on the NI diet (60µmol/L) compared to the mice on the CI (50µmol/L) diet. Also, there was a significantly higher level of serum iron for the HFE$^{-/-}$ ($p<0.01$) and HJV$^{-/-}$ and DKO ($p<0.001$ for both) mice compared to WT mice on the NI diet, as was seen in Figure 3.1A. However there were no significant changes in serum iron levels between the genotypes on the CI diet (Figure 3.3 left).

Serum ferritin levels were significantly higher in HJV$^{-/-}$ and DKO mice (1425 and 1675µg/L) ($p<0.001$ for both) compared to WT (320µg/L) on the NI diet and in HJV$^{-/-}$ and DKO mice (2500 and 2450 µg/L) ($p<0.001$ for both) compared to WT (1000µg/L) on the CI diet (Figure 3.3 middle). This represented a 4.5-fold higher level in HJV$^{-/-}$ mice and a 5.2-fold higher level for DKO mice on the NI diet compared to WT mice on the same diet and a 2.5-fold higher level for both HJV$^{-/-}$ and DKO mice on the CI diet compared to WT mice. Within each genotype, there was also a significant higher level of serum ferritin between mice on the NI and CI diets ($p<0.001$ for WT, HJV$^{-/-}$, and DKO and $p<0.01$ for HFE$^{-/-}$).

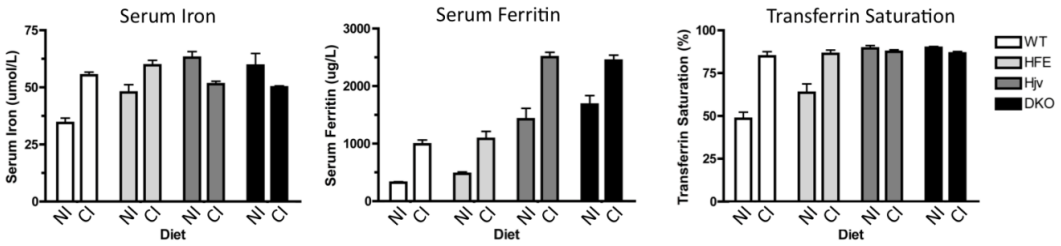

Figure 3.3: Serum analysis of high iron diet challenged mice. Male mice (n=8) were placed on a 2% carbonyl iron (CI) enriched iron diet (5.6g iron per kg) for 4 weeks before sacrifice and were compared to mice on a normal iron (NI) diet (225mg iron per kg). Serum iron levels were significantly higher in $HFE^{-/-}$ ($p<0.01$) and in $HJV^{-/-}$ and DKO ($p<0.001$) mice compared to WT on the NI diet. There were no significant changes in the serum iron level between any genotype mice on the CI diet. There was significantly higher levels of serum iron in the WT mice between the NI and CI diets ($p<0.001$) and in the $HFE^{-/-}$ mice between the NI and CI diets ($p<0.05$). Serum ferritin levels were significantly higher in $HJV^{-/-}$ and DKO mice ($p<0.001$ for both) compared to WT mice on the NI diet and in the $HJV^{-/-}$ and DKO mice ($p<0.001$) compared to WT mice on the CI diet. Within each genotype, serum ferritin was significantly higher for the CI diet compared to the NI diet ($p<0.001$ for WT, $HJV^{-/-}$, and DKO and $p<0.01$ for HFE KO). Transferrin saturation levels were significantly higher in both WT and $HFE^{-/-}$ mice on the CI diet compared to the NI diet ($p<0.001$ for both). Transferrin saturation was significantly higher in $HFE^{-/-}$, $HJV^{-/-}$, and DKO mice ($p<0.001$ for all) compared to WT on the NI diet. Transferrin was fully saturated for all mice genotypes on the CI diet.

Transferrin saturation was significantly higher in $HFE^{-/-}$ (65%) and in $HJV^{-/-}$ and DKO (both 89%) compared to WT (50%) mice on the NI diet ($p<0.001$ for all). For both WT and $HFE^{-/-}$ mice on the NI diet, there was significantly lower levels of transferrin saturation compared to the matched genotype mice on the CI diet (85% for both) ($p<0.001$ for both). Transferrin saturation was already at a maximum level in both $HJV^{-/-}$ and DKO mice on the NI diet and the CI diet

challenge showed no change in transferrin saturation which was 88% for both (Figure 3.3 right).

3.5.4 Hepcidin mRNA expression is severely attenuated in DKO mice, particularly when normalized to liver iron loading

Next, Hepc mRNA expression levels in the liver were compared between male mice on the NI and CI diets (Figure 3.4A). As expected, Hepc mRNA expression was significantly higher in all the genotypes on the CI diet compared to the NI diet ($p<0.001$ for WT, $HFE^{-/-}$, and $HJV^{-/-}$ and $p<0.01$ for DKO) with a 3.5 to 4-fold induction being observed in each genotype except $HJV^{-/-}$ which had a 10-fold induction between the diets. There was significantly lower levels of Hepc mRNA expression in the $HJV^{-/-}$ ($p<0.01$) and DKO ($p<0.05$) compared to the WT mice on the NI diet, as well as in the $HJV^{-/-}$ and DKO ($p<0.001$ for both) compared to the WT mice on the CI diet. Both WT and $HFE^{-/-}$ levels of Hepc mRNA expression on either diet were similar. There were no differences between the $HJV^{-/-}$ and DKO mice Hepc mRNA expression levels on either the NI or CI diets (Figure 3.4A right).

Liver and spleen iron contents for both heme bound and non-heme bound iron were determined via the sensitive technique of atomic absorption spectrometry (Figure 3.4B). For all genotypes, liver iron content was significantly higher in the CI diet compared to the matched genotype mice on the NI diet ($p<0.05$ for WT, and $p<0.001$ for $HFE^{-/-}$, $HJV^{-/-}$, and DKO). This represents an 11-fold higher level for WT mice, a 7.4-fold higher level for $HFE^{-/-}$ mice, and a 3-fold higher level for $HJV^{-/-}$ and DKO mice between the CI and NI diets. (Figure 3.4B left). As seen with the ferrozine assay, liver iron was higher for $HFE^{-/-}$ (3.8-fold) and significantly higher for $HJV^{-/-}$ (12-fold) ($p<0.01$) and DKO (15-fold) ($p<0.001$) as compared to WT mice on the NI diet mice. The same significantly higher levels of liver iron content was seen in the mice on the CI diet as well, however the higher level for $HFE^{-/-}$ mice compared to WT was now significant as well ($p<0.001$).

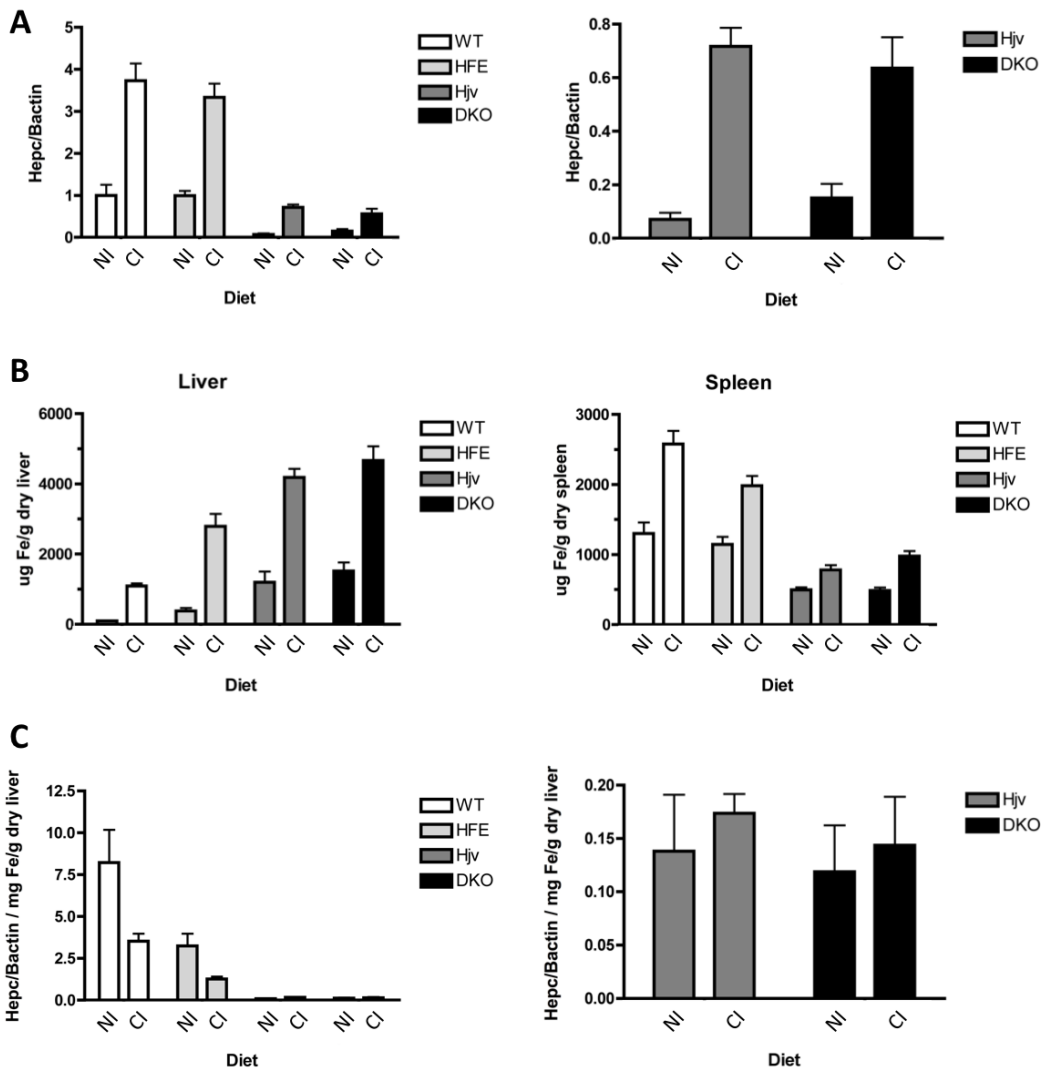

Figure 3.4: Hepcidin mRNA expression and tissue iron loading in mice fed a high dietary iron diet. (A) Hepc mRNA expression was standardized to β-actin control gene and reported as fold changes from WT mice on the NI diet. Within each genotype, Hepc mRNA expression was significantly higher for the mice on the CI diet as compared to the NI diet ($p<0.001$ for all except DKO ($p<0.01$)). There were no differences between either WT and $HFE^{-/-}$ on either diet or between $HJV^{-/-}$ and DKO on either diet. There was significantly lower Hepc mRNA expression in $HJV^{-/-}$ ($p<0.01$) and DKO ($p<0.05$) on the NI diet compared to WT and in $HJV^{-/-}$ and DKO ($p<0.001$) on the CI diet compared to WT mice. (B) Atomic absorption spectrometry determination of heme and non-heme bound iron of the liver (left) and spleen (right) is reported as µg iron per g of dry tissue

weight. For all genotypes there was significantly higher levels of liver iron content in mice on the CI diet compared to the NI diet ($p<0.001$ for all except WT ($p<0.05$)). Also, there was significantly higher levels of liver iron content in $HFE^{-/-}$ (p=ns) and further in $HJV^{-/-}$ ($p<0.01$) and still further in DKO ($p<0.001$) mice on the NI diet compared to WT and also for all genotype mice on the CI diet compared to WT ($p<0.001$). Splenic iron content was significantly higher for the CI diet mice compared to NI diet mice within each genotype ($p<0.001$ for WT and $HFE^{-/-}$ and $p<0.05$ for DKO). Also, iron loading was lower in $HFE^{-/-}$ and significantly lower in $HJV^{-/-}$ and DKO ($p<0.001$) on the NI diet compared to WT and also for the CI diet with the change from WT to $HFE^{-/-}$ now being significant ($p<0.01$). (C) Hepc mRNA expression normalized to the β-actin control gene and then compared to liver iron loading and reported as mRNA fold changes per mg iron per g of dry liver weight. For WT and $HFE^{-/-}$ mice, there were lower levels of expression for the CI diet mice as compared to the NI diet (left) ($p<0.001$ for WT) but there were no changes in mRNA expression per mg iron in either $HJV^{-/-}$ or DKO mice (right). There was significantly lower expression level in all genotypes as compared to WT on the NI diet ($p<0.001$) and also a significantly lower expression for the $HFE^{-/-}$ ($p<0.05$) and for the $HJV^{-/-}$ and DKO ($p<0.01$) on the CI diet as compared to WT mice.

Splenic iron loading was lower in $HFE^{-/-}$ and significantly 2.6-fold for $HJV^{-/-}$ and DKO ($p<0.001$ for both) for the NI diet as compared to WT. It also was significantly lower in $HFE^{-/-}$ (1.3-fold) ($p<0.01$) and in $HJV^{-/-}$ and DKO (3-fold) ($p<0.001$) on the CI diet as compared to WT. Within each genotype, splenic iron content was between 1.7 and 2-fold higher for the CI diet as compared to the NI diet (Figure 3.4B right). This was significantly higher iron content between the diets for WT and $HFE^{-/-}$ ($p<0.001$ for both) and DKO ($p<0.05$) mice.

Data comparing hepatic Hepc mRNA expression relative to liver iron loading are shown in Figure 3.4C. For mice on the NI diet, there was a significant 2.6-fold

lower expression of Hepc mRNA per mg liver iron in $HFE^{-/-}$ ($p<0.001$) and a massive 64-fold lower expression in $HJV^{-/-}$ and DKO mice ($p<0.001$ for both) as compared to WT. For the mice on the CI diet, there was a significant 2.7-fold lower expression in $HFE^{-/-}$ mice ($p<0.05$) and a 23-fold lower expression in $HJV^{-/-}$ and DKO mice ($p<0.01$) as compared to WT. For WT and $HFE^{-/-}$ mice there was lower Hepc mRNA expression for the mice on the CI diet as compared to the NI diet, but only the WT change of 2.4-fold showed significance ($p<0.001$). Interestingly, there was no difference between NI and CI diet Hepc mRNA expression in either $HJV^{-/-}$ or DKO mice (Figure 3.4C right).

3.5.5 BMP6, SMAD7, and Id1 mRNA expression is attenuated in DKO mice

Expression of other genes (*BMP6*, *SMAD7*, and *Id1*) that are positively regulated by dietary iron and the BMP/SMAD signalling cascade were determined via qPCR and normalized to the β-actin control gene expression (Figure 3.5). BMP6 is further regulated by hepatic iron stores. BMP6 mRNA expression was higher in $HFE^{-/-}$ (1.8-fold) and significantly in $HJV^{-/-}$ and DKO (3.6-fold) ($p<0.001$) as compared to WT mice on the NI diet. Also, a significant 1.6-fold higher expression was seen in $Hjv^{-/-}$ and DKO ($p<0.001$) as compared to WT on the CI diet. Within each genotype, there was significantly higher levels of BMP6 mRNA expression ($p<0.001$ WT, $HJV^{-/-}$, and DKO, and $p<0.01$ $HFE^{-/-}$) for mice on the CI diet as compared to the NI diet. This represents a 4.3-fold higher expression level for WT and a 2-fold higher level for all other genotypes (Figure 3.5 left). For SMAD7 mRNA expression, WT mice showed a significant 5.2-fold induction between NI and CI diets ($p<0.001$) (Figure 3.5 middle). $HFE^{-/-}$ mice had an attenuated 1.9-fold induction between diets. $HJV^{-/-}$ and DKO mice had no SMAD7 mRNA induction on the CI diet when compared to WT CI diet mice ($p<0.001$ for all). This was also seen in Id1 mRNA expression (Figure 3.5 right). In WT there was a robust 20-fold induction from the NI diet to the CI diet ($p<0.001$) which was eliminated in both $HFE^{-/-}$ and $HJV^{-/-}$ mice with only a 3-fold induction and further depressed in DKO mice with a 1.9-fold induction of Id1 mRNA expression.

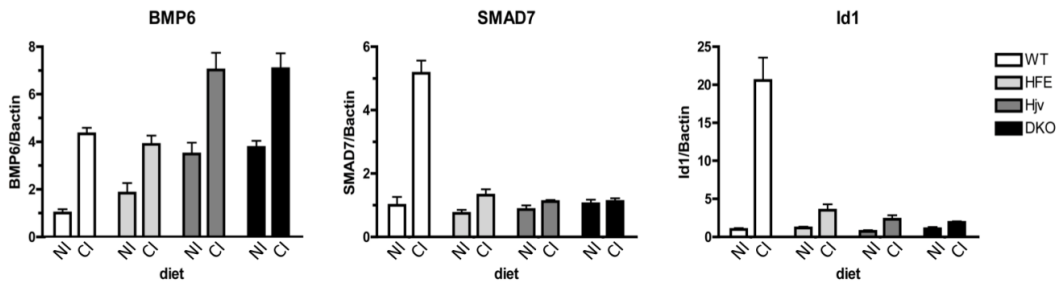

Figure 3.5: BMP6, SMAD7, and Id1 mRNA expression in dietary iron challenged mice. mRNA expression levels of BMP6, SMAD7, and Id1 were measured via qPCR and reported as fold changes from WT mice on the NI diet with respect to β-actin control gene expression. BMP6 mRNA expression (left) was significantly higher for each genotype on the CI diet as compared to the NI diet ($p<0.001$ for all except $HFE^{-/-}$ ($p<0.01$)). WT and $HFE^{-/-}$ mice were similar in both NI and CI diet BMP6 mRNA expression levels. There was significantly higher expression in $HJV^{-/-}$ and DKO ($p<0.001$) as compared to WT mice on the NI diet and also in the CI diet between these two genotypes ($p<0.001$). SMAD7 mRNA expression (middle) was significantly higher in WT mice on the CI diet as compared to the NI diet ($p<0.001$) but was completely attenuated in all other genotypes. Id1 mRNA expression (right) was also only significantly higher for WT mice ($p<0.001$) on the CI diet as compared to the NI diet, slightly but not significantly higher in $HFE^{-/-}$ and $HJV^{-/-}$ mice on the CI diet compared to the NI diet, but completely attenuated in DKO mice.

3.6 DISCUSSION

In order to study the crosstalk between the hepatic iron and serum iron sensing pathways that regulate Hepc expression, a novel mouse model was generated. This global knockout mouse of both the *HFE* and *HJV* genes allowed for a closer investigation into the upstream regulation of Hepc, especially with mice challenged with high dietary iron intake in the form of a 2% carbonyl iron enriched diet. Since it is known that there is variation in iron loading between different mouse backgrounds because of each strain's specific genetic makeup

[145], both knockout genotypes were previously backcrossed onto a pure C57BL/6 background. Then these pure C57BL/6 $HFE^{-/-}$ and $HJV^{-/-}$ mice were crossed together to generate the double knockout (DKO) mouse and compared to WT mice. Only male mice were used in experiments, since there are gender based differences in iron loading [143], and sacrificed at 10 weeks of age. This time point was selected because it is known that iron levels rapidly increase from birth to 5 weeks of age then plateau by 10 weeks of age for $HFE^{-/-}$ mice [144]. $HFE^{-/-}$ mice are phenotypically like hereditary hemochromatosis (HH) type I patients [142], who present with iron loading in the fourth to fifth decade of life [4], and $HJV^{-/-}$ mice are like HH type IIA patients, who present with iron loading in the second decade of life [75, 133]. Therefore, the 10 week time point is sufficient to see maximal $HFE^{-/-}$ iron loading, as well as $HJV^{-/-}$ iron loading since $HJV^{-/-}$ mice accumulate iron more rapidly than $HFE^{-/-}$ mice.

Serum parameters were investigated in the single knockouts and DKO mice and compared to WT. As expected serum iron was higher in $HFE^{-/-}$ and even higher in $HJV^{-/-}$ as compared to WT. DKO mice did not show a difference in serum iron levels as compared to $HJV^{-/-}$ (Figure 3.1A left). Serum ferritin levels also were higher in $HJV^{-/-}$ and ever higher in DKO mice as compared to WT (Figure 3.1A middle). There was no significant difference between serum ferritin for the $HJV^{-/-}$ and DKO mice and the small difference is most likely due to mouse to mouse variations. Surprisingly WT and $HFE^{-/-}$ mice had similar serum ferritin levels, despite $HFE^{-/-}$ having more iron loading (an increase in serum iron, an increase in transferrin saturation, and more iron in the liver). Transferrin saturation was also higher in $HFE^{-/-}$, $HJV^{-/-}$, and DKO as compared to WT mice. WT transferrin saturation of 50% is comparable to other groups finding for pure C57BL/6 mice, though saturation values vary greatly [143, 145, 146]. Again, there was no difference between $HJV^{-/-}$ and DKO mice, even though DKO transferrin saturation was slightly higher than $HJV^{-/-}$ (Figure 3.1A right).

Complete blood count (CBC) was performed on the mice, with specific interest in red blood cell count (RBC), hemoglobin concentration (HGB), hematocrit percentage (HCT), and platelet count (PLT) (Figure 3.1B). RBC, HGB, and HCT were identical for all genotypes and PLT was slightly lower for $HFE^{-/-}$, $HJV^{-/-}$, and DKO as compared to WT. It is not surprising that there are no differences in blood parameters between the mice, since there are no erythropoiesis phenotypes reported for the $HFE^{-/-}$ and $HJV^{-/-}$ mice, so none were expected for the DKO mouse either. However, since these mice have inappropriately low levels of hepcidin, which plays a key role in erythropoiesis, and substantial iron loading, the possibility of a phenotype had to be examined.

To determine liver iron loading, a ferrozine assay was performed to determine the amount of non-heme bound iron in the liver. Figure 3.2 showed that both $HJV^{-/-}$ and DKO mice had equally massive iron loading of the liver as compared to both WT and $HFE^{-/-}$ mice. $HJV^{-/-}$ liver iron loading is in line with how HH type IIA (due to mutations in *HJV*) patients develop more iron more rapidly, which is stored within ferritin in the liver. $HFE^{-/-}$ mice had more liver iron than WT mice, which is not unexpected. The difference in liver iron loading in $HFE^{-/-}$ and $HJV^{-/-}$ mice was also not unexpected since it is known that HH type I (due to mutations in *HFE*) is a milder form of HH than type IIA [17]. Interestingly, DKO mice showed equal liver iron loading to the $HJV^{-/-}$ mice. This could be due to the liver already being saturated with iron and unable to store any more within ferritin but is more likely due to the HJV and HFE signalling pathways having crosstalk.

In order to determine if these DKO mice could be stressed to show a more overt phenotype, they along with the single knockout and WT mice, were placed on a high iron diet. Mice were split into two groups at 6 weeks of age and were either maintained on a standard iron diet containing approximately 225mg iron per kg (normal iron – NI), or placed on an enriched iron diet of 2% carbonyl iron (5.6g iron per kg) (CI). Serum iron parameters were measured looking for specific

differences between the mice on the NI and CI diets, as well as differences between the genotypes on the CI diet.

Serum iron levels for mice on the NI diet (Figure 3.3 left) were the same as the dietary unchallenged mice in Figure 3.1A (left), in that serum iron was higher in $HFE^{-/-}$ as compared to WT and higher still in $HJV^{-/-}$ and DKO as compared to WT. DKO and $HJV^{-/-}$ mice still had similar values for serum iron in the repeated measurements in Figure 3.3 (left). With the CI diet challenge both WT and $HFE^{-/-}$ mice had higher levels of serum iron as compared to the genotype matched mice on the NI diet. Interestingly on the CI diet both $HJV^{-/-}$ and DKO mice showed a minor lower level of serum iron levels as compared to the NI diet. This is unexpected since the CI diets should have either raised the serum iron levels in these two genotypes (as seen with WT and $HFE^{-/-}$ mice) or there should have been no change (since serum iron levels are already significantly high and probably have reached a plateau). Serum ferritin levels also followed the trend from the dietary unchallenged mice in Figure 3.1A (middle), however in the repeated experiment (Figure 3.3 middle) the serum ferritin values were much higher for $HJV^{-/-}$ and DKO mice. This is most likely due to an inappropriate dilution factor selected by my collaborator such that the machine used to measure serum ferritin levels was beyond its threshold. That being said, in the repeated NI diet experiment, serum ferritin in the $HFE^{-/-}$ was slightly higher than WT mice and in the $HJV^{-/-}$ and DKO there was a significantly more serum ferritin as compared to WT (Figure 3.3 middle). Not surprisingly, the WT and $HFE^{-/-}$ mice on the CI diet had similar serum ferritin levels and there was still no difference in $HJV^{-/-}$ and DKO mice serum ferritin levels. Also not surprisingly, with the CI diet all genotypes showed higher levels of serum ferritin as compared to the matched genotype mice on the NI diet. Transferrin saturation levels again resembled the unchallenged mice in Figure 3.1A (right), but the $HJV^{-/-}$ mice on a NI diet had the same transferrin saturation levels as DKO mice as opposed to $HFE^{-/-}$ mice (Figure 3.3 right). This is more logical than the initial findings in Figure 3.1A (right) since it is known that $HJV^{-/-}$ mice have more severe iron loading than $HFE^{-/-}$ and

therefore should have higher transferrin saturation levels. All genotypes on the CI diet showed transferrin saturation of approximately 90%, indicating that this is the maximal transferrin saturation for C57BL/6 background mice.

Since there were still no apparent differences in the serum biochemistry parameters of the DKO mice compared to the $HJV^{-/-}$, even when the mice were challenged with a high iron diet, liver Hepc mRNA levels were investigated. Only *HAMP1* (Hep gene) was analyzed via qPCR since in mice which have 2 *HAMP* genes only *HAMP1* has been implicated in iron metabolism [147]. WT and $HFE^{-/-}$ mice on either the NI or CI diet had almost identical levels of Hepc mRNA expression (Figure 3.4A left). While this result was surprising, it has been documented that absolute levels of Hepc mRNA in the liver of $HFE^{-/-}$ mice can be similar to WT. However when considering the increased liver iron content and serum iron levels the expression is inappropriately low [148]. Therefore in Figure 3.4C (left), it can be seen that in $HFE^{-/-}$ mice on either the NI or CI diet Hepc mRNA expression normalized to liver iron content is lower as compared to WT. $HJV^{-/-}$ and DKO mice had significantly blunted Hepc mRNA expression in the liver on either the NI or CI diet compared to WT (Figure 3.4A right). There is no difference between $HJV^{-/-}$ and DKO mice on either NI or CI diet. Both genotypes respond to the CI diet with an increase in Hepc mRNA expression compared to NI diet, as would be expected with the increase of iron from the diet. The expression of Hepc mRNA is further depressed when normalized to liver iron load (Figure 3.4C right), with $HJV^{-/-}$ and DKO mice having more than a 50-fold lower expression of Hepc mRNA as compared to WT.

Looking at liver iron loading in the dietary iron challenged mice with the more sensitive technique of atomic absorption spectrometry (both heme and non-heme bound iron can be detected), showed the same trend as the unchallenged mice in Figure 3.2. Liver iron content in mice on the NI diet was greater in $HFE^{-/-}$ and further increased in $HJV^{-/-}$ and DKO as compared to WT (Figure 3.4B left). All genotypes responded to the CI diet as expected, in that liver iron content was

greater for mice on the CI diet as compared to the NI diet. Again, there was no difference between $HJV^{-/-}$ and DKO liver iron content for the mice on either the NI or CI diet. Splenic iron content was lower as expected for $HFE^{-/-}$ and further in $HJV^{-/-}$ and DKO mice as compared to WT on both the NI and CI diets (Figure 3.4B right). Within each genotype, there was more splenic iron loading for mice on the CI diet as compared to mice on the NI diet, which was expected. Unlike the liver, which is the primary storage tissue for excess iron [50], the spleen contains a large number of macrophages. These macrophages are the body's recycling center for iron since they are the site that heme bound iron within senescent red blood cells is released back into circulation [43]. In mice with misregulation of Hepc ($HFE^{-/-}$, $HJV^{-/-}$, and DKO in Figure 3.4A) liver iron content increases because it is attempting to store the excess iron coming from the diet. At the same time, splenic iron content decreases due to the lack of circulating Hepc (because of the knockout of the upstream iron sensors). Therefore the FPN expressed on the macrophages is not degraded and can export iron from the cells which has the overall effect of decreasing splenic iron content.

Lastly, other known targets of the liver specific BMP/SMAD pathway, which is critical in signalling to Hepc, was investigated. mRNA expression of BMP6, SMAD7, and Id1 in the liver was determined by qPCR since these are known downstream targets of pSMAD1/5/8 [67]. BMP6 is further positively regulated by hepatic iron stores [67]. This was confirmed here in Figure 3.5 (left) since there was greater BMP6 mRNA expression in $HFE^{-/-}$ as compared to WT and a further higher expression in $HJV^{-/-}$ and DKO mice on the NI diet, which was coupled with the same higher liver iron content between the genotypes (Figure 3.4B left). Also, this trend of the stepped higher BMP6 mRNA expression from WT to DKO was seen in the CI diet as well, with $HJV^{-/-}$ and DKO mice showing the same level of BMP6 mRNA expression. This was not surprising since both genotypes showed the same level of liver iron loading as well. Both SMAD7 and Id1 are known to be regulated directly by pSMAD1/5/8 and pSMAD4 binding to their promoters to induce gene expression [67]. In Figure 3.5 (middle) SMAD7

mRNA expression in the liver of WT mice was positively regulated by the CI diet as compared to the NI diet. This is due to the fact that the pSMAD signalling cascade is intact and is responding to dietary iron from both the serum iron pathway (as seen by the elevation in serum iron and transferrin saturation in $HFE^{-/-}$ mice (Figure 3.3)) and the hepatic iron pathway (as seen by the elevation in hepatic iron loading in $HJV^{-/-}$ mice (Figure 3.4B left)). However, in $HFE^{-/-}$ mice, there was only a mild 1.5-fold induction of SMAD7 mRNA expression on the CI diet as compared to the NI diet. This indicates that the lack of HFE results in a decrease in pSMAD1/5/8 and therefore decreased SMAD7 mRNA induction. In $HJV^{-/-}$ mice, the reduction in SMAD7 mRNA induction between NI and CI diets is further reduced. This was not unexpected since it is known that the pSMAD cascade is central in HJV iron dependent signalling. Interestingly, there was a complete abolishment of SMAD7 mRNA expression for the DKO mice on the CI diet as compared to the NI diet. This indicates that when both HFE and HJV are eliminated, there is no signalling through the pSMAD cascade via either the serum iron or hepatic iron pathways. This is also true for Id1 mRNA expression (Figure 3.5 right) since WT mice showed a robust 20-fold induction on the CI diet as compared to the NI diet, $HFE^{-/-}$ and $HJV^{-/-}$ showed a blunted 3-fold induction and DKO showed a further attenuated 1.5-fold induction of Id1 mRNA in the liver.

In conclusion, this data taken together indicates that there is crosstalk in the iron dependent regulation of systemic iron homeostasis mediated by HFE and HJV. The most likely candidate for the point of convergence between the two pathways is at the level of pSMAD1/5/8. This will need to be confirmed in future studies both *in vitro* using recombinant HFE and HJV proteins in a human liver cell line with a reporter assay for the Hepc promoter as well as *in vivo* on protein levels on these novel combined HFE and HJV knockout mice.

CHAPTER 4

FINAL CONCLUSIONS

It is known that systemic iron regulation within the body is a tightly controlled process. This ensures that there is enough iron to meet the cellular and systemic needs, while not allowing excess iron to cause damage to individual cells, tissue, and organs as a whole. Humans, like all other mammals, have evolved an elaborate system to sense and maintain iron levels and it was the discovery of a peptide hormone known as hepcidin that was found to play a pivotal role in systemic iron homeostasis. While many of the upstream regulatory elements of hepcidin have been determined in the last ten years, questions still remain, of which here we looked at two in particular.

In Chapter 2, the surprising link that was found previously *in vivo* between dietary iron intake, and therefore iron loading, and SERPIN B3 mRNA expression was investigated *in vitro*. The *in vivo* work indicated that iron was directly affecting the transcription of SERPIN B3. To investigate the mechanism of induction, an *in vitro* reporter assay to test the iron responsiveness of the SERPIN B3 promoter was generated. While robust iron-dependent transcriptional regulation was seen *in vivo*, results could not be recapitulated *in vitro*. Even with testing a secondary effect of unshielded iron, that being the generation of oxidative stress, no induction of the SERPIN B3 promoter was detected. Unfortunately a functional role of SERPIN B3 as an upstream regulator of hepcidin via the HJV/BMP6/TMPRSS6 pathway was neither proven nor disproven. However it seems unlikely that the serine protease TMPRSS6 would be affected by the cysteine-specific SERPIN B3 serine protease inhibitor.

In Chapter 3, the crosstalk in the iron sensing pathways that are critical in signalling to hepcidin and therefore maintaining systemic iron homeostasis was investigated. To do this, a novel knockout mouse with global deletions in both the *HFE* and *HJV* genes was generated. It was determined that serum iron parameters were no different in the $HJV^{-/-}$ and DKO mice but were significantly higher than in WT mice. Hepatic iron as well as splenic iron loading were also indistinguishable between the $HJV^{-/-}$ and DKO mice. Not surprisingly, hepcidin

mRNA expression in the liver, already severely attenuated in $HJV^{-/-}$ mice as compared to WT, was comparable to DKO mice. These three findings taken together indicate that the iron sensing pathways that HFE and HJV belong to must have a degree of crosstalk since DKO mice did not show a further increase in iron loading or further decrease in hepcidin expression. Further experiments into other genes that are regulated by the same BMP/SMAD pathway as hepcidin indicated the likely intersection point of the two iron pathways. SMAD7 and Id1 mRNA expression levels in the liver, while significantly attenuated in both $HFE^{-/-}$ and $HJV^{-/-}$ mice are further depressed in DKO mice, indicating that the crosstalk between the pathways is likely via pSMAD1/5/8. However, future experiments will need to be conducted to confirm this conclusion.

CHAPTER 5: **REFERENCES**

1. Sheftel, A.D., A.B. Mason, and P. Ponka, *The long history of iron in the Universe and in health and disease.* Biochim Biophys Acta, 2012. **1820**(3): p. 161-87.
2. McDonald, I.S., G. C.; Zijlstra, A. A.; Matsunaga, N.;; Matsuura, M.; Kraemer, K. E.; Bernard-Salas, J.; Markwick, A. J. , *Rusty Old Stars: A Source of the Missing Interstellar Iron?* The Astrophysical Journal Letters, 2010. **717** (2): p. L92–L97.
3. Lavoisier, A., *Opuscles physiques et chemiques*. 1774, Paris, France: Chez Durand, Didot, Esprit.
4. Sebastiani, G. and K. Pantopoulos, *Disorders associated with systemic or local iron overload: from pathophysiology to clinical practice.* Metallomics, 2011. **3**(10): p. 971-86.
5. Toyokuni, S., *Iron-induced carcinogenesis: the role of redox regulation.* Free Radic Biol Med, 1996. **20**(4): p. 553-66.
6. Papanikolaou, G. and K. Pantopoulos, *Iron metabolism and toxicity.* Toxicol Appl Pharmacol, 2005. **202**(2): p. 199-211.
7. Hentze, M.W., M.U. Muckenthaler, and N.C. Andrews, *Balancing acts: molecular control of mammalian iron metabolism.* Cell, 2004. **117**(3): p. 285-97.
8. Haber, F.W., J., *The catalytic decompostion of hydrogen peroxide by iron salts.* Proc. R. Soc. Land, 1934. **147**: p. 332-351.
9. Fenton, H.J.H., *Oxidation of tartaric acid in the presence of iron.* J. Chem. Soc, 1894. **65**: p. 899-910.
10. Emerit, J., C. Beaumont, and F. Trivin, *Iron metabolism, free radicals, and oxidative injury.* Biomed Pharmacother, 2001. **55**(6): p. 333-9.
11. Mello-Filho, A.C. and R. Meneghini, *Iron is the intracellular metal involved in the production of DNA damage by oxygen radicals.* Mutat Res, 1991. **251**(1): p. 109-13.
12. Gutteridge, J.M., D.A. Rowley, and B. Halliwell, *Superoxide-dependent formation of hydroxyl radicals and lipid peroxidation in the presence of iron salts. Detection of 'catalytic' iron and anti-oxidant activity in extracellular fluids.* Biochem J, 1982. **206**(3): p. 605-9.
13. Gkouvatsos, K., G. Papanikolaou, and K. Pantopoulos, *Regulation of iron transport and the role of transferrin.* Biochim Biophys Acta, 2012. **1820**(3): p. 188-202.
14. Wang, J. and K. Pantopoulos, *Regulation of cellular iron metabolism.* Biochem J, 2011. **434**(3): p. 365-81.
15. Hentze, M.W., et al., *Two to tango: regulation of Mammalian iron metabolism.* Cell, 2010. **142**(1): p. 24-38.
16. Green, R., et al., *Body iron excretion in man: a collaborative study.* Am J Med, 1968. **45**(3): p. 336-53.

17. De Domenico, I., D. McVey Ward, and J. Kaplan, *Regulation of iron acquisition and storage: consequences for iron-linked disorders.* Nat Rev Mol Cell Biol, 2008. **9**(1): p. 72-81.
18. Pantopoulos, K., et al., *Mechanisms of mammalian iron homeostasis.* Biochemistry, 2012. **51**(29): p. 5705-24.
19. Ponka, P. and C.N. Lok, *The transferrin receptor: role in health and disease.* Int J Biochem Cell Biol, 1999. **31**(10): p. 1111-37.
20. Andrews, N.C., *Forging a field: the golden age of iron biology.* Blood, 2008. **112**(2): p. 219-30.
21. Han, O., *Molecular mechanism of intestinal iron absorption.* Metallomics, 2011. **3**(2): p. 103-9.
22. McKie, A.T., et al., *An iron-regulated ferric reductase associated with the absorption of dietary iron.* Science, 2001. **291**(5509): p. 1755-9.
23. Gunshin, H., et al., *Cybrd1 (duodenal cytochrome b) is not necessary for dietary iron absorption in mice.* Blood, 2005. **106**(8): p. 2879-83.
24. Gunshin, H., et al., *Cloning and characterization of a mammalian proton-coupled metal-ion transporter.* Nature, 1997. **388**(6641): p. 482-8.
25. Gunshin, H., et al., *Slc11a2 is required for intestinal iron absorption and erythropoiesis but dispensable in placenta and liver.* J Clin Invest, 2005. **115**(5): p. 1258-66.
26. Shayeghi, M., et al., *Identification of an intestinal heme transporter.* Cell, 2005. **122**(5): p. 789-801.
27. Severance, S. and I. Hamza, *Trafficking of heme and porphyrins in metazoa.* Chem Rev, 2009. **109**(10): p. 4596-616.
28. Khan, A.A. and J.G. Quigley, *Heme and FLVCR-related transporter families SLC48 and SLC49.* Mol Aspects Med, 2013. **34**(2-3): p. 669-82.
29. Koskenkorva-Frank, T.S., et al., *The complex interplay of iron metabolism, reactive oxygen species, and reactive nitrogen species: Insights into the potential of various iron therapies to induce oxidative and nitrosative stress.* Free Radic Biol Med, 2013. **65C**: p. 1174-1194.
30. Abboud, S. and D.J. Haile, *A novel mammalian iron-regulated protein involved in intracellular iron metabolism.* J Biol Chem, 2000. **275**(26): p. 19906-12.
31. Donovan, A., et al., *Positional cloning of zebrafish ferroportin1 identifies a conserved vertebrate iron exporter.* Nature, 2000. **403**(6771): p. 776-81.
32. McKie, A.T., et al., *A novel duodenal iron-regulated transporter, IREG1, implicated in the basolateral transfer of iron to the circulation.* Mol Cell, 2000. **5**(2): p. 299-309.
33. Donovan, A., et al., *The iron exporter ferroportin/Slc40a1 is essential for iron homeostasis.* Cell Metab, 2005. **1**(3): p. 191-200.
34. Vulpe, C.D., et al., *Hephaestin, a ceruloplasmin homologue implicated in intestinal iron transport, is defective in the sla mouse.* Nat Genet, 1999. **21**(2): p. 195-9.
35. De Domenico, I., et al., *Ferroxidase activity is required for the stability of cell surface ferroportin in cells expressing GPI-ceruloplasmin.* EMBO J, 2007. **26**(12): p. 2823-31.

36. Schade, A.L. and L. Caroline, *An iron-binding component in human blood plasma.* Science, 1946. **104**(2702): p. 340.
37. Aisen, P., A. Leibman, and J. Zweier, *Stoichiometric and site characteristics of the binding of iron to human transferrin.* J Biol Chem, 1978. **253**(6): p. 1930-7.
38. Dautry-Varsat, A., A. Ciechanover, and H.F. Lodish, *pH and the recycling of transferrin during receptor-mediated endocytosis.* Proc Natl Acad Sci U S A, 1983. **80**(8): p. 2258-62.
39. Bali, P.K., O. Zak, and P. Aisen, *A new role for the transferrin receptor in the release of iron from transferrin.* Biochemistry, 1991. **30**(2): p. 324-8.
40. Ohgami, R.S., et al., *Identification of a ferrireductase required for efficient transferrin-dependent iron uptake in erythroid cells.* Nat Genet, 2005. **37**(11): p. 1264-9.
41. Brissot, P., et al., *Non-transferrin bound iron: a key role in iron overload and iron toxicity.* Biochim Biophys Acta, 2012. **1820**(3): p. 403-10.
42. Levy, J.E., et al., *Transferrin receptor is necessary for development of erythrocytes and the nervous system.* Nat Genet, 1999. **21**(4): p. 396-9.
43. Knutson, M. and M. Wessling-Resnick, *Iron metabolism in the reticuloendothelial system.* Crit Rev Biochem Mol Biol, 2003. **38**(1): p. 61-88.
44. Harris, Z.L., et al., *Targeted gene disruption reveals an essential role for ceruloplasmin in cellular iron efflux.* Proc Natl Acad Sci U S A, 1999. **96**(19): p. 10812-7.
45. Epsztejn, S., et al., *H-ferritin subunit overexpression in erythroid cells reduces the oxidative stress response and induces multidrug resistance properties.* Blood, 1999. **94**(10): p. 3593-603.
46. Hintze, K.J. and E.C. Theil, *Cellular regulation and molecular interactions of the ferritins.* Cell Mol Life Sci, 2006. **63**(5): p. 591-600.
47. Theil, E.C., *Ferritin: at the crossroads of iron and oxygen metabolism.* J Nutr, 2003. **133**(5 Suppl 1): p. 1549S-53S.
48. Ferreira, C., et al., *Early embryonic lethality of H ferritin gene deletion in mice.* J Biol Chem, 2000. **275**(5): p. 3021-4.
49. Zhang, Y., et al., *Lysosomal proteolysis is the primary degradation pathway for cytosolic ferritin and cytosolic ferritin degradation is necessary for iron exit.* Antioxid Redox Signal, 2010. **13**(7): p. 999-1009.
50. Fleming, R.E. and P. Ponka, *Iron overload in human disease.* N Engl J Med, 2012. **366**(4): p. 348-59.
51. Park, C.H., et al., *Hepcidin, a urinary antimicrobial peptide synthesized in the liver.* J Biol Chem, 2001. **276**(11): p. 7806-10.
52. Valore, E.V. and T. Ganz, *Posttranslational processing of hepcidin in human hepatocytes is mediated by the prohormone convertase furin.* Blood Cells Mol Dis, 2008. **40**(1): p. 132-8.
53. Palaneeswari, M.S., et al., *Hepcidin-minireview.* J Clin Diagn Res, 2013. **7**(8): p. 1767-71.
54. Lesbordes-Brion, J.C., et al., *Targeted disruption of the hepcidin 1 gene results in severe hemochromatosis.* Blood, 2006. **108**(4): p. 1402-5.

55. Nicolas, G., et al., *Severe iron deficiency anemia in transgenic mice expressing liver hepcidin.* Proc Natl Acad Sci U S A, 2002. **99**(7): p. 4596-601.
56. Nemeth, E., et al., *Hepcidin regulates cellular iron efflux by binding to ferroportin and inducing its internalization.* Science, 2004. **306**(5704): p. 2090-3.
57. Nicolas, G., et al., *The gene encoding the iron regulatory peptide hepcidin is regulated by anemia, hypoxia, and inflammation.* J Clin Invest, 2002. **110**(7): p. 1037-44.
58. Gao, J., et al., *Interaction of the hereditary hemochromatosis protein HFE with transferrin receptor 2 is required for transferrin-induced hepcidin expression.* Cell Metab, 2009. **9**(3): p. 217-27.
59. Schmidt, P.J., et al., *The transferrin receptor modulates Hfe-dependent regulation of hepcidin expression.* Cell Metab, 2008. **7**(3): p. 205-14.
60. West, A.P., Jr., et al., *Mutational analysis of the transferrin receptor reveals overlapping HFE and transferrin binding sites.* J Mol Biol, 2001. **313**(2): p. 385-97.
61. Giannetti, A.M., et al., *Mechanism for multiple ligand recognition by the human transferrin receptor.* PLoS Biol, 2003. **1**(3): p. E51.
62. Chen, J., et al., *HFE modulates transferrin receptor 2 levels in hepatoma cells via interactions that differ from transferrin receptor 1-HFE interactions.* J Biol Chem, 2007. **282**(51): p. 36862-70.
63. Johnson, M.B. and C.A. Enns, *Diferric transferrin regulates transferrin receptor 2 protein stability.* Blood, 2004. **104**(13): p. 4287-93.
64. Kautz, L., et al., *BMP/Smad signaling is not enhanced in Hfe-deficient mice despite increased Bmp6 expression.* Blood, 2009. **114**(12): p. 2515-20.
65. Corradini, E., et al., *Bone morphogenetic protein signaling is impaired in an HFE knockout mouse model of hemochromatosis.* Gastroenterology, 2009. **137**(4): p. 1489-97.
66. Ramey, G., J.C. Deschemin, and S. Vaulont, *Cross-talk between the mitogen activated protein kinase and bone morphogenetic protein/hemojuvelin pathways is required for the induction of hepcidin by holotransferrin in primary mouse hepatocytes.* Haematologica, 2009. **94**(6): p. 765-72.
67. Kautz, L., et al., *Iron regulates phosphorylation of Smad1/5/8 and gene expression of Bmp6, Smad7, Id1, and Atoh8 in the mouse liver.* Blood, 2008. **112**(4): p. 1503-9.
68. Andriopoulos, B., Jr., et al., *BMP6 is a key endogenous regulator of hepcidin expression and iron metabolism.* Nat Genet, 2009. **41**(4): p. 482-7.
69. Babitt, J.L., et al., *Bone morphogenetic protein signaling by hemojuvelin regulates hepcidin expression.* Nat Genet, 2006. **38**(5): p. 531-9.
70. Truksa, J., et al., *The distal location of the iron responsive region of the hepcidin promoter.* Blood, 2007. **110**(9): p. 3436-7.

71. Truksa, J., et al., *Different regulatory elements are required for response of hepcidin to interleukin-6 and bone morphogenetic proteins 4 and 9.* Br J Haematol, 2007. **139**(1): p. 138-47.
72. Silvestri, L., et al., *The serine protease matriptase-2 (TMPRSS6) inhibits hepcidin activation by cleaving membrane hemojuvelin.* Cell Metab, 2008. **8**(6): p. 502-11.
73. Meynard, D., et al., *Lack of the bone morphogenetic protein BMP6 induces massive iron overload.* Nat Genet, 2009. **41**(4): p. 478-81.
74. Wang, R.H., et al., *A role of SMAD4 in iron metabolism through the positive regulation of hepcidin expression.* Cell Metab, 2005. **2**(6): p. 399-409.
75. Huang, F.W., et al., *A mouse model of juvenile hemochromatosis.* J Clin Invest, 2005. **115**(8): p. 2187-91.
76. Nemeth, E., et al., *IL-6 mediates hypoferremia of inflammation by inducing the synthesis of the iron regulatory hormone hepcidin.* J Clin Invest, 2004. **113**(9): p. 1271-6.
77. Wrighting, D.M. and N.C. Andrews, *Interleukin-6 induces hepcidin expression through STAT3.* Blood, 2006. **108**(9): p. 3204-9.
78. Tanno, T., et al., *High levels of GDF15 in thalassemia suppress expression of the iron regulatory protein hepcidin.* Nat Med, 2007. **13**(9): p. 1096-101.
79. Tanno, T., et al., *Identification of TWSG1 as a second novel erythroid regulator of hepcidin expression in murine and human cells.* Blood, 2009. **114**(1): p. 181-6.
80. Pinto, J.P., et al., *Erythropoietin mediates hepcidin expression in hepatocytes through EPOR signaling and regulation of C/EBPalpha.* Blood, 2008. **111**(12): p. 5727-33.
81. Camaschella, C., *Understanding iron homeostasis through genetic analysis of hemochromatosis and related disorders.* Blood, 2005. **106**(12): p. 3710-7.
82. Feder, J.N., et al., *A novel MHC class I-like gene is mutated in patients with hereditary haemochromatosis.* Nat Genet, 1996. **13**(4): p. 399-408.
83. Papanikolaou, G., et al., *Mutations in HFE2 cause iron overload in chromosome 1q-linked juvenile hemochromatosis.* Nat Genet, 2004. **36**(1): p. 77-82.
84. Roetto, A., et al., *Mutant antimicrobial peptide hepcidin is associated with severe juvenile hemochromatosis.* Nat Genet, 2003. **33**(1): p. 21-2.
85. Camaschella, C., et al., *The gene TFR2 is mutated in a new type of haemochromatosis mapping to 7q22.* Nat Genet, 2000. **25**(1): p. 14-5.
86. Wallace, D.F., et al., *Combined deletion of Hfe and transferrin receptor 2 in mice leads to marked dysregulation of hepcidin and iron overload.* Hepatology, 2009. **50**(6): p. 1992-2000.
87. Pietrangelo, A., *The ferroportin disease.* Blood Cells Mol Dis, 2004. **32**(1): p. 131-8.

88. Drakesmith, H., et al., *Resistance to hepcidin is conferred by hemochromatosis-associated mutations of ferroportin.* Blood, 2005. **106**(3): p. 1092-7.
89. Liu, X.B., F. Yang, and D.J. Haile, *Functional consequences of ferroportin 1 mutations.* Blood Cells Mol Dis, 2005. **35**(1): p. 33-46.
90. De Domenico, I., et al., *The molecular basis of ferroportin-linked hemochromatosis.* Proc Natl Acad Sci U S A, 2005. **102**(25): p. 8955-60.
91. Roy, C.N. and N.C. Andrews, *Anemia of inflammation: the hepcidin link.* Curr Opin Hematol, 2005. **12**(2): p. 107-11.
92. Weinstein, D.A., et al., *Inappropriate expression of hepcidin is associated with iron refractory anemia: implications for the anemia of chronic disease.* Blood, 2002. **100**(10): p. 3776-81.
93. Ganz, T., *Hepcidin, a key regulator of iron metabolism and mediator of anemia of inflammation.* Blood, 2003. **102**(3): p. 783-8.
94. Finberg, K.E., et al., *Mutations in TMPRSS6 cause iron-refractory iron deficiency anemia (IRIDA).* Nat Genet, 2008. **40**(5): p. 569-71.
95. Gettings, P., *Serpin structure, mechanism, and function.* Chem Rev, 2002. **102**: p. 4751-4804.
96. Gatto, M., et al., *Serpins, immunity and autoimmunity: old molecules, new functions.* Clin Rev Allergy Immunol, 2013. **45**(2): p. 267-80.
97. Potempa, J., E. Korzus, and J. Travis, *The serpin superfamily of proteinase inhibitors: structure, function, and regulation.* J Biol Chem, 1994. **269**(23): p. 15957-60.
98. Silverman, G.A., et al., *The serpins are an expanding superfamily of structurally similar but functionally diverse proteins. Evolution, mechanism of inhibition, novel functions, and a revised nomenclature.* J Biol Chem, 2001. **276**(36): p. 33293-6.
99. Khan, M.S., et al., *Serpin Inhibition Mechanism: A Delicate Balance between Native Metastable State and Polymerization.* J Amino Acids, 2011. **2011**: p. 606797.
100. Huntington, J.A., *Serpin structure, function and dysfunction.* J Thromb Haemost, 2011. **9 Suppl 1**: p. 26-34.
101. Vidalino, L., et al., *SERPINB3, apoptosis and autoimmunity.* Autoimmun Rev, 2009. **9**(2): p. 108-12.
102. Izuhara, K., et al., *Recent progress in understanding the diversity of the human ov-serpin/clade B serpin family.* Cell Mol Life Sci, 2008. **65**(16): p. 2541-53.
103. Irving, J.A., et al., *Phylogeny of the serpin superfamily: implications of patterns of amino acid conservation for structure and function.* Genome Res, 2000. **10**(12): p. 1845-64.
104. Remold-O'Donnell, E., *The ovalbumin family of serpin proteins.* FEBS Lett, 1993. **315**(2): p. 105-8.
105. Kato, H. and T. Torigoe, *Radioimmunoassay for tumor antigen of human cervical squamous cell carcinoma.* Cancer, 1977. **40**(4): p. 1621-8.

106. Cataltepe, S., et al., *Co-expression of the squamous cell carcinoma antigens 1 and 2 in normal adult human tissues and squamous cell carcinomas.* J Histochem Cytochem, 2000. **48**(1): p. 113-22.
107. Uemura, Y., et al., *Circulating serpin tumor markers SCCA1 and SCCA2 are not actively secreted but reside in the cytosol of squamous carcinoma cells.* Int J Cancer, 2000. **89**(4): p. 368-77.
108. Pontisso, P., et al., *Overexpression of squamous cell carcinoma antigen variants in hepatocellular carcinoma.* Br J Cancer, 2004. **90**(4): p. 833-7.
109. Turato, C., et al., *SERPINB3 modulates TGF-beta expression in chronic liver disease.* Lab Invest, 2010. **90**(7): p. 1016-23.
110. Hashimoto, K., et al., *Effect of SCCA1 and SCCA2 on the suppression of TNF-alpha-induced cell death by impeding the release of mitochondrial cytochrome c in an oral squamous cell carcinoma cell line.* Tumour Biol, 2005. **26**(4): p. 165-72.
111. Schick, C., et al., *Cross-class inhibition of the cysteine proteinases cathepsins K, L, and S by the serpin squamous cell carcinoma antigen 1: a kinetic analysis.* Biochemistry, 1998. **37**(15): p. 5258-66.
112. Rodust, P.M., et al., *UV-induced squamous cell carcinoma--a role for antiapoptotic signalling pathways.* Br J Dermatol, 2009. **161 Suppl 3**: p. 107-15.
113. Murakami, A., et al., *Squamous cell carcinoma antigen suppresses radiation-induced cell death.* Br J Cancer, 2001. **84**(6): p. 851-8.
114. Katagiri, C., et al., *Serpin squamous cell carcinoma antigen inhibits UV-induced apoptosis via suppression of c-JUN NH2-terminal kinase.* J Cell Biol, 2006. **172**(7): p. 983-90.
115. Zhong, Z., Z. Wen, and J.E. Darnell, Jr., *Stat3: a STAT family member activated by tyrosine phosphorylation in response to epidermal growth factor and interleukin-6.* Science, 1994. **264**(5155): p. 95-8.
116. Ahmed, S.T. and J.E. Darnell, Jr., *Serpin B3/B4, activated by STAT3, promote survival of squamous carcinoma cells.* Biochem Biophys Res Commun, 2009. **378**(4): p. 821-5.
117. Suminami, Y., et al., *Inhibition of apoptosis in human tumour cells by the tumour-associated serpin, SCC antigen-1.* Br J Cancer, 2000. **82**(4): p. 981-9.
118. Sebastiani, G., et al., *Accelerated CCl4-induced liver fibrosis in Hjv-/- mice, associated with an oxidative burst and precocious profibrogenic gene expression.* PLoS One, 2011. **6**(9): p. e25138.
119. Casanovas, G., et al., *Bone morphogenetic protein (BMP)-responsive elements located in the proximal and distal hepcidin promoter are critical for its response to HJV/BMP/SMAD.* J Mol Med (Berl), 2009. **87**(5): p. 471-80.
120. Morgenstern, J.P. and H. Land, *Advanced mammalian gene transfer: high titre retroviral vectors with multiple drug selection markers and a complementary helper-free packaging cell line.* Nucleic Acids Res, 1990. **18**(12): p. 3587-96.

121. Moore, P.L., S. Ong, and T.J. Harrison, *Squamous cell carcinoma antigen 1-mediated binding of hepatitis B virus to hepatocytes does not involve the hepatic serpin clearance system.* J Biol Chem, 2003. **278**(47): p. 46709-17.
122. Velasco, G., et al., *Matriptase-2, a membrane-bound mosaic serine proteinase predominantly expressed in human liver and showing degrading activity against extracellular matrix proteins.* J Biol Chem, 2002. **277**(40): p. 37637-46.
123. Sun, D. and M. Nassal, *Stable HepG2- and Huh7-based human hepatoma cell lines for efficient regulated expression of infectious hepatitis B virus.* J Hepatol, 2006. **45**(5): p. 636-45.
124. Suminami, Y., et al., *Promoter analyses of SCC antigen genes.* Biochim Biophys Acta, 2005. **1727**(3): p. 208-12.
125. Hamada, K., et al., *Molecular cloning of human squamous cell carcinoma antigen 1 gene and characterization of its promoter.* Biochim Biophys Acta, 2001. **1518**(1-2): p. 124-31.
126. Verga Falzacappa, M.V., et al., *STAT3 mediates hepatic hepcidin expression and its inflammatory stimulation.* Blood, 2007. **109**(1): p. 353-8.
127. Giannelli, G., et al., *Clinical role of tissue and serum levels of SCCA antigen in hepatocellular carcinoma.* Int J Cancer, 2005. **116**(4): p. 579-83.
128. Ryter, S.W. and R.M. Tyrrell, *The heme synthesis and degradation pathways: role in oxidant sensitivity. Heme oxygenase has both pro- and antioxidant properties.* Free Radic Biol Med, 2000. **28**(2): p. 289-309.
129. Ganz, T., *Systemic iron homeostasis.* Physiol Rev, 2013. **93**(4): p. 1721-41.
130. Canonne-Hergaux, F., et al., *Comparative studies of duodenal and macrophage ferroportin proteins.* Am J Physiol Gastrointest Liver Physiol, 2006. **290**(1): p. G156-63.
131. Ramey, G., et al., *Hepcidin targets ferroportin for degradation in hepatocytes.* Haematologica, 2010. **95**(3): p. 501-4.
132. Drakesmith, H. and A.M. Prentice, *Hepcidin and the iron-infection axis.* Science, 2012. **338**(6108): p. 768-72.
133. Ganz, T. and E. Nemeth, *Hepcidin and disorders of iron metabolism.* Annu Rev Med, 2011. **62**: p. 347-60.
134. Zhou, X.Y., et al., *HFE gene knockout produces mouse model of hereditary hemochromatosis.* Proc Natl Acad Sci U S A, 1998. **95**(5): p. 2492-7.
135. Bridle, K.R., et al., *Disrupted hepcidin regulation in HFE-associated haemochromatosis and the liver as a regulator of body iron homoeostasis.* Lancet, 2003. **361**(9358): p. 669-73.
136. Kawabata, H., et al., *Expression of hepcidin is down-regulated in TfR2 mutant mice manifesting a phenotype of hereditary hemochromatosis.* Blood, 2005. **105**(1): p. 376-81.

137. Fleming, R.E., et al., *Targeted mutagenesis of the murine transferrin receptor-2 gene produces hemochromatosis.* Proc Natl Acad Sci U S A, 2002. **99**(16): p. 10653-8.
138. Wallace, D.F., et al., *First phenotypic description of transferrin receptor 2 knockout mouse, and the role of hepcidin.* Gut, 2005. **54**(7): p. 980-6.
139. Courselaud, B., et al., *Strain and gender modulate hepatic hepcidin 1 and 2 mRNA expression in mice.* Blood Cells Mol Dis, 2004. **32**(2): p. 283-9.
140. Leboeuf, R.C., D. Tolson, and J.W. Heinecke, *Dissociation between tissue iron concentrations and transferrin saturation among inbred mouse strains.* J Lab Clin Med, 1995. **126**(2): p. 128-36.
141. Gkouvatsos, K., Fillebeen, C., et al., *Iron-dependent regulation of hepcidin in Hjv-/- mice: Evidence that hemojuvelin is dispensable for sensing body iron levels.* PLoS One, 2013.
142. Levy, J.E., et al., *The C282Y mutation causing hereditary hemochromatosis does not produce a null allele.* Blood, 1999. **94**(1): p. 9-11.
143. Vujic Spasic, M., et al., *Physiologic systemic iron metabolism in mice deficient for duodenal Hfe.* Blood, 2007. **109**(10): p. 4511-7.
144. Subramaniam, V.N., et al., *Hepatic iron deposition does not predict extrahepatic iron loading in mouse models of hereditary hemochromatosis.* Am J Pathol, 2012. **181**(4): p. 1173-9.
145. Fleming, R.E., et al., *Mouse strain differences determine severity of iron accumulation in Hfe knockout model of hereditary hemochromatosis.* Proc Natl Acad Sci U S A, 2001. **98**(5): p. 2707-11.
146. Chaudhury, C., et al., *Accelerated transferrin degradation in HFE-deficient mice is associated with increased transferrin saturation.* J Nutr, 2006. **136**(12): p. 2993-8.
147. Lou, D.Q., et al., *Functional differences between hepcidin 1 and 2 in transgenic mice.* Blood, 2004. **103**(7): p. 2816-21.
148. Ahmad, K.A., et al., *Decreased liver hepcidin expression in the Hfe knockout mouse.* Blood Cells Mol Dis, 2002. **29**(3): p. 361-6.